HHS Public Access

Author manuscript

Curr Protoc Cell Biol. Author manuscript; available in PMC 2017 January 17.

Published in final edited form as:

Curr Protoc Cell Biol. 2013 March ; CHAPTER 4: Unit4.21. doi:10.1002/0471143030.cb0421s58.

Photoactivated Localization Microscopy (PALM) of Adhesion Complexes

Hari Shroff[1], **Helen White**[2], and **Eric Betzig**[2]

[1]National Institute of Biomedical Imaging and Bioengineering, National Institutes of Health, Bethesda, Maryland [2]Howard Hughes Medical Institute, Janelia Farm Research Campus, Ashburn, Virginia

Abstract

Key to understanding a protein's biological function is the accurate determination of its spatial distribution inside a cell. Although fluorescent protein markers allow the targeting of specific proteins with molecular precision, much of this information is lost when the resultant fusion proteins are imaged with conventional, diffraction-limited optics. In response, several imaging modalities that are capable of resolution below the diffraction limit (~200 nm) have emerged. Here, both single- and dual-color superresolution imaging of biological structures using photoactivated localization microscopy (PALM) are described. The examples discussed focus on adhesion complexes: dense, protein-filled assemblies that form at the interface between cells and their substrata. A particular emphasis is placed on the instrumentation and photoactivatable fluorescent protein (PA-FP) tags necessary to achieve PALM images at ~20 nm resolution in 5 to 30 min in fixed cells.

Keywords

PALM; superresolution; adhesion complex; fluorescent proteins

INTRODUCTION

The accurate determination of a protein's spatial distribution inside a cell is often intimately related to its function. Fluorescence microscopy allows the imaging and subsequent analysis of protein distributions inside cellular specimens, and fluorescent proteins allow an investigator to genetically target a protein with molecular precision. Unfortunately, valuable information is lost when conventional fluorescence microscopy is used to image the resulting protein fusions, because diffraction limits the smallest features that can be resolved with an optical microscope to ~200 nm.

In response, a number of far-field superresolution imaging modalities that are capable of breaking the diffraction barrier have emerged (Gustafsson, 2000, 2005; Betzig et al., 2006; Hess et al., 2006; Rust et al., 2006; Willig et al., 2006). Photoactivated localization microscopy (PALM; Betzig et al., 2006) relies on the stochastic activation, localization, and bleaching of single photoswitchable molecules, and initially used photoactivatable fluorescent proteins (PA-FPs, reviewed in Wiedenmann and Nienhaus, 2006; also see *UNIT*

21.6) at the high density and localization precision necessary to provide images at > 10× higher spatial resolution than corresponding diffraction-limited images (Fig. 4.21.1). Several other methods (Hess et al., 2006; Rust et al., 2006) have relied upon similar characteristics of photoswitchable molecules to provide superresolution, albeit at lower density and spatial resolution.

This unit describes the application of PALM to the imaging of adhesion complexes, transmembrane protein assemblies that form attachment points between the cytoskeleton and substratum and that are critical in cell migration (Zamir and Geiger, 2001). Adhesion complexes represent a particularly good test system for PALM: as many types of proteins (>90) are concentrated in structures as small as 0.5 μm (Zaidel-Bar et al., 2007), conventional fluorescence imaging is clearly inadequate to resolve internal adhesion complex structure (Fig. 4.21.1).

Several considerations are important in achieving the best PALM images of adhesion complexes. First, the choice of photoactivatable tag dictates the maximum achievable resolution; this consideration is discussed in Strategic Planning. Second, although PALM instrumentation is relatively straightforward, some additional knowledge in designing a PALM system is helpful and is covered in Basic Protocol 1. A method that uses PALM instrumentation in combination with appropriate sample preparation techniques to provide superresolution images of the adhesion protein paxillin is described in Basic Protocol 2. Finally, Basic Protocol 3 describes the additional steps necessary to undertake dual-color PALM-imaging of two adhesion complex proteins (vinculin and α-actinin).

STRATEGIC PLANNING

PALM is a single-molecule technique: the raw data consist of a stack of thousands of individual frames, each containing diffraction-limited fluorescence images of single photoswitchable molecules present in the sample. The fluorescence images of each molecule are analyzed to determine their centers with high precision, and the resultant information is used to generate a high-resolution PALM image of the positions of the molecules. The resolution of PALM is thus dependent on *localization precision*: how well the position of each single molecule can be determined from its diffraction-limited image. Perhaps more subtle but equally important in determining the ultimate PALM resolution is the *density* of molecules present in the sample (see Background Information for a detailed discussion of factors influencing PALM resolution). The localization precision depends on maximizing the signal-to-noise ratio in each image, a characteristic that in turn depends on maximizing the collected photons from each photoswitchable molecule and minimizing the background fluorescence. These instrumentation considerations are discussed in Basic Protocol 1. However, the localization precision also depends on the total number of photons emitted by each molecule before it bleaches, an intrinsic property of the molecule. Furthermore, taking full advantage of the molecular density in each sample is contingent on the *contrast ratio* of the molecule, another intrinsic property (see Background Information). It is the authors' belief that the correct choice of photoswitchable molecule is the single most important factor in obtaining high-quality PALM images—that choice is the subject of this section.

All PALM experiments currently conducted by the authors use PA-FPs as the photoswitchable molecules, instead of exogenously introduced caged dyes—such as caged fluorescein, resorufin, or rhodamine (Mitchison et al., 1998; Betzig et al., 2006)—that are conjugated to antibodies or proteins via small-molecule labeling strategies (Chen and Ting, 2005; Giepmans et al., 2006). PA-FPs have the tremendous advantage of being exquisitely specific; by genetically fusing a PA-FP to a target protein and transfecting the cellular sample, the investigator is assured that there is a 1:1 correspondence between a detected molecule and its target, and thus avoids the nonspecific binding that arises with dye-conjugated antibodies or proteins. PA-FPs also better approximate the size of a target protein, whereas antibodies can introduce considerable uncertainty due to their size (10 to 20 nm, depending on whether both primary and secondary antibodies are used). Due to their small size, PA-FPs can achieve higher densities in principle than antibodies, and thus offer increased PALM resolution. Finally, PA-FP genes are readily available as plasmid DNAs and are easily ligated to DNA coding for the protein target. Some of the potential downsides of PA-FPs are mentioned in Critical Parameters and Troubleshooting. Recent efforts have revealed that many commercially available dyes may be photoswitched at high intensities and with proper chemicals added to the imaging buffer (Heilemann et al., 2008; Dempsey et al., 2011); these dyes are not discussed further in this chapter.

Most PA-FPs can be broken up into two classes: those that switch colors, e.g., from a green fluorescent state to an orange state (EosFP, Wiedenmann et al., 2004; KikGR, Tsutsui et al., 2005; and Kaede, Ando et al., 2002) upon photoactivation, and those that switch from a dark state to a bright fluorescent state (e.g., PAmCherry1, Subach et al., 2009; PA-GFP, Patterson and Lippincott-Schwartz, 2002; or Dronpa, Ando et al., 2004) upon photoactivation. After testing candidates from both classes, the authors have concluded that EosFP is the best choice for PALM, due both to the high number of emitted photons before bleaching (>1000 photons, providing localization precision to ~10 nm; Shroff et al., 2007) and the greatly increased contrast ratio ($>10^3$, providing both increased localization precision and enabling PALM-imaging of densely-labeled specimens) relative to other PA-FPs (see Fig. 4.21.2 and Background Information). Also, as the activated state of Eos has a fluorescence emission spectrum that peaks at 580 nm, emission filters can be chosen to minimize cellular autofluorescence (more prevalent in the 450 to 550 nm region, overlapping with the emission spectrum of PA-GFP and Dronpa). Unlike KikGR, EosFP can be completely photoconverted from its green state to the orange state, a characteristic that is essential for the serial dual-label PALM procedure described in Basic Protocol 3. Finally, any FP-labeling strategy is prone to aggregation artifacts, and these problems can be exacerbated if the label is present in nonmonomeric form. EosFP is currently available in tandem-dimeric and monomeric forms (mEos2, McKinney et al., 2009).

Despite these factors, there may be situations where it is advantageous to use other PA-FPs as the PALM label. For example, in dual-label PALM-imaging (Shroff et al., 2007), it is necessary to use EosFP in conjunction with another PA-FP (either Dronpa or PS-CFP2; Chudakov et al., 2004, 2007). If the investigator must use an FP or fluorophore as a conventional, diffraction-limited label, and the label has significant spectral overlap with EosFP, it may be necessary to use a different PA-FP as the PALM label (although it is better

to first pick the PALM label and then the diffraction-limited label, as the choice of PA-FPs is considerably more limited).

PREPARING PALM INSTRUMENTATION

Instead of a conventional step-by-step protocol, this section describes the instrumentation necessary for PALM. As PALM is inherently a single-molecule technique, standard methods for suppressing background fluorescence and for detecting relatively faint single-molecule emissions apply (Weiss, 1999). In particular, total internal reflection (TIRF) microscopy (Axelrod, 2001; *UNIT 4.12*) is advantageous for PALM, because the evanescent excitation wave penetrates <200 nm into the sample, leading to extreme rejection of the background fluorescence common in cellular samples, thus facilitating the detection of single fluorescent molecules. TIRF is also a widefield technique, implying that many molecules per frame can be imaged simultaneously, thus vastly increasing the acquisition speed. TIRF is particularly appropriate for imaging adhesion complexes, as these structures are located close (within 100 nm) to the substrate and are thus within the TIRF excitation region. Note that TIRF is not a requirement for PALM, as certain specimens (such as bacteria) are sufficiently thin that autofluorescence does not impede the localization of single molecules illuminated in epifluorescence. Other studies (Hess et al., 2006; Egner et al., 2007) have reported epifluorescence PALM imaging, albeit with lower resolution images than those reported here, and 3D PALM on thicker samples frequently employs epi-illumination (Huang et al., 2008; Juette et al., 2008). We note that multiphoton (York et al., 2011) or plane-illumination (Cella Zanacchi et al., 2011) strategies improve single-molecule detection in thicker samples, but are outside the scope of this article.

With some minor modifications and additions to the existing hardware, it is possible to adapt an existing commercial TIRF microscope for PALM (Shroff et al., 2007; Fig. 4.21.3). Free-space coupling (i.e., without an optical fiber) of appropriate excitation and activation lasers into the microscope ensures that enough power is delivered to the sample, and permits fast PALM imaging. Using a microscope objective with as high a numerical aperture (NA) as possible allows high photon collection efficiency and facilitates TIRF. Choosing an appropriate electron-multiplying charge-coupled device (EMCCD) camera is an important factor in imaging the faint emissions from single fluorescent molecules, as is choosing the best available excitation, emission, and dichroic filters. Finally, a computer with acquisition software, image acquisition board, and a large hard drive is important for acquiring and storing the large PALM acquisition stacks. The authors have tried to be as general as possible in describing the major components, but have given specific recommendations when relevant.

Materials

Optical table (Technical Manufacturing Corporation)

Inverted fluorescence microscope (e.g., Olympus IX-81) assembly, including:

Brightfield and DIC optics

Capability for TIRF illumination

High NA objective lenses (1.45 NA, 1.49 NA, or 1.65 NA) with matching coverslips, and immersion media

Internal magnification lens (optional, depending on objective magnification)

Additional magnification before camera (optional, depending on objective magnification)

Mercury *or* xenon lamp

Mechanically stable stage and sample mount

Appropriate excitation and activation lasers and optics (beam expanders, neutral density filters, half-wave plates, and dichroic beamsplitters) for coupling lasers into the TIRF microscope path

Appropriate excitation, emission, and dichroic filters

Acousto-optic tunable filter (AA Opto-Electronic, AA-AOTFnC-VIS)

EMCCD camera (see step 12 for details)

Computer with appropriate control software (see step 14 for details)

Computer with appropriate analysis software (see step 16 for details)

Set up inverted fluorescence microscope with associated optics and stage

1 Bolt a research-quality fluorescence microscope to an optical table in order to minimize unwanted vibrations and prevent relative motion between the microscope and table. Use a microscope with ports for epi- and TIRF-illumination, and for mounting an EMCCD camera for detection. Use a brightfield condenser and differential interference contrast (DIC) optics for imaging samples conventionally before PALM-imaging, and a mercury or xenon lamp to aid in initial examination of the specimen with diffraction-limited epifluorescence imaging prior to PALM-imaging.

Some of these components are illustrated in Fig.4.21.3.

The authors use an Olympus IX-81 as the base microscope for PALM. The microscope is bolted to a 4

× 8–ft optical table, large enough to comfortably fit both the microscope and the associated lasers and TIRF optics described below. The back-port of the microscope is fitted with the Olympus U-DP dual-port tube to switch between widefield epi-illumination (with a mercury or xenon lamp) and laser illumination (for TIRF). The microscope is also fitted with a polarizer, analyzer, and Nomarski DIC prisms for transmitted DIC imaging. Given the sample chamber design described below, a long working-distance condenser is necessary to prevent the condenser from physically colliding with the sample chamber. The authors use an NA 0.55, 27-mm working-distance condenser (Olympus, IX2-LWUCD). Finally, the authors recommend using an adjustable, focusable lamp housing (Olympus, IX-HLSH100), as they have obtained more uniform DIC illumination with this device than with the standard lamp housing (U-LH100L-3-5), which cannot be focused or adjusted.

2 Minimize sample drift by bolting a mechanically stable, rigid stage to the microscope frame.

If a motorized stage with linear encoders is used, it is easy to repeatedly return to the same position on the sample, a feature that is useful for marking appropriately transfected cells.

Although most stages come with a variety of inserts for convenient sample loading, use of clips to hold down the sample should be avoided. A more stable option is to design a baseplate that can be bolted to the stage (Fig. 4.21.4), and a threaded coverslip holder that contains the sample (Fig. 4.21.5) and that can be attached firmly to the baseplate.

The authors use an MS-2000 XY stage with linear encoders (ASI). The stage is bolted to the IX-81 frame directly above the objective, and a baseplate holding the sample chamber (that holds the sample-containing coverslip) is bolted to the stage.

TIRF excitation scheme

3 Select appropriate laser wavelengths for activating and exciting the PA-FP chosen as the PALM-label. Use solid-state diode lasers to provide ample power at a reasonable cost.

Almost all available PA-FPs are activated efficiently at 405 nm; thus a laser with this wavelength is required. For PALM-imaging EosFP, a 561-nm laser is also advised, as it can be used for excitation of the activated (orange) state (an Argon/Krypton mixed gas laser has a 568-nm laser line, which is closer to the 580-nm absorption peak of EosFP, but this laser is also considerably more expensive than a 561-nm diode laser).

A 488-nm laser is also very useful for imaging the inactive state of EosFP (i.e., for imaging the distribution of EosFP at the diffraction limit before PALM-imaging and determining which cells are expressing the fusion protein at the desired levels), and is essential for exciting the activated (green) state of Dronpa or PA-GFP.

The authors use a 50-mW 405-nm laser (Coherent, 405-50C) for activation, a 150-mW 561-nm laser (Crystalaser, GCL-150-561) to excite the active state of EosFP, and a 50-mW 488-nm laser (Newport Spectra-Physics Cyan Scientific Laser) for imaging the inactive state of EosFP or the activated state of Dronpa. The characteristics from these diode lasers are not always as advertised: the mode quality may be poor and the intensity may drift slightly. For PALM, these characteristics are not critical, as long as enough power is available to excite or activate molecules in the desired region at the sample. However, a particularly poor beam profile may be difficult to focus at the back focal plane (BFP) of the objective without clipping, may be hard to co-align with the other laser beams, and may thus impede successful TIRF illumination of the specimen. The authors have noticed that the beam quality from the 405-nm laser is somewhat poor; utilizing a spatial filter (a telescope system consisting of 12-mm and 50-mm focal length lenses separated by the sum of their focal lengths, and a 10-μm pinhole positioned at the intermediate image plane between the two lenses) immediately after the laser output cleans up the beam profile considerably and improves the ease with which the sample is TIRF-activated.

4 Free-space couple all lasers into a TIRF-capable illumination microscope port. Use neutral density filters and half-wave plates (FIL) to control the intensity and polarization [important for

maximum transmission through the acousto-optic tunable filter (AOTF) element discussed below] of each beam. In addition, use a narrow bandpass excitation filter (Semrock LL01-488-25) with the 488-nm laser to reduce emission noise. Use beam expanders (BE) after each laser to yield a common beam diameter (important for establishing an excitation/activation region of common size at the sample).

One possible coupling scheme is shown in Figure 4.21.6 (reproduced from the supporting information in Shroff et al., 2007). Activation and excitation lasers are indicated by their respective wavelengths. Beam expanders are made from achromatic lenses (Edmund Scientific) mounted in ½-in. diameter lens tubes (Thorlabs).

5 Combine the 488-nm and 561-nm excitation beams with a dichroic beamsplitter (DC) prior to passage through an acousto-optic tunable filter (AOTF), then combine excitation beams with the 405-nm activation beam with a second dichroic beamsplitter (DC).

An FF-506-Di02-25 × 36 (Semrock) dichroic beamsplitter is used to combine 488-nm and 561-nm beams before the AOTF.

The AOTF serves as a rapid switch to select between wavelengths, and can also be synchronized to the frame acquisition cycle of the detection EMCCD (discussed further below) in order to minimize photobleaching during the read-out period between frames.

Synchronization can be easily achieved by connecting the Fire output signal from the EMCCD detector to the AOTF input. The AOTF output beam in turn is combined with the 405-nm activation beam using a second dichroic beamsplitter (Semrock, FF458-Di02-25 ×36). The reason for combining the activation beam with the excitation beams in a position downstream of the AOTF is that the AOTF used does not transmit wavelengths <450 nm efficiently. Goniometer (Thorlabs, cat. no. GN05)–mounted glass windows (CVI Inc.; 2 windows/goniometer, each 12.5-mm diameter, 5-mm thick) are used to fine-adjust the position of each beam (TX, TY), thereby facilitating their mutual overlap, and the assorted dichroic beamsplitters and mirrors in the system provide further

adjustment of the position and direction of propagation.

Although it is also possible to couple all three lasers into a commercial TIRF illumination unit using an appropriate multi-wavelength fiber (e.g., the PointSource kineFlex fiber), these fibers transmit at best 50% to 60% of the incident laser light, and typically <50% due to the poor mode quality of the beams from the diode lasers. This results in excitation intensities that are too low for the fastest PALM acquisitions.

6 Once excitation and activation beams are co-aligned, bring them to a focus at the back focal plane (BFP) of the objective used for TIRF excitation and activation.

This can be done with the aid of two lenses, FL (focusing lens) and CL (collimating lens; Fig. 4.21.6 and Fig. 4.21.7).

7 Position the entire laser illumination system relative to the imaging microscope such that the BFP of lens CL is coincident with the front focal plane of a 200-mm relay lens internal to the microscope (Fig. 4.21.7). By doing so, the focus created by lens FL is imaged at the BFP of the microscope objective.

With this geometry, the image of the focus can be moved within the objective BFP using the translating mirror (TM), thereby switching between epi and TIRF modes of laser excitation without affecting the position of the spot at the sample. Lastly, by switching between lenses CL of differing focal length, and by changing the magnification of the BEs, the diameter of the beam launched into the microscope can be changed, resulting in a change in the excitation/activation spot size, and thus the laser intensity, at the sample. Small spots can be used to achieve fast single-molecule frame rates (~10 to 20 msec), or large spots can be used to image at slower rates but over larger fields of view.

The commercial Olympus IX-81 TIRF Illuminator can be conveniently modified and stripped down to conform with the guidelines presented above. This system is usually attached to the rear port of the IX-81. The authors use the U-DP attachment (Olympus) to switch between arc lamp and TIRF illumination (Fig. 4.21.7), but only the 200-mm relay lens in the TIRF

illuminator is necessary—the entire fiber-coupling assembly can be removed.

Excitation, dichroic, and emission filters

8 Carefully choose excitation, dichroic, and emission filters to maximize the fluorescence signal while rejecting excitation light.

The use of lasers can sometimes preclude the use of excitation filters, as the excitation light is already quasi-monochromatic. However, occasionally, broadband emission noise generated in the laser cavity or autofluorescence generated elsewhere in the optical path necessitates the use of narrowband excitation filters.

9 Select the dichroic filter to simultaneously reflect both activation and excitation wavelengths (so that time is not wasted in switching dichroics between activation and excitation steps during the PALM-imaging), while transmitting the much weaker fluorescent emissions with high efficiency.

10 Finally, select the emission filter to provide >6 OD suppression of excitation light and activation light, while maximally transmitting the fluorescence emission.

Bandpass emission filters have been found to better suppress the excitation light than longpass filters, such as Raman edge filters. Dichroic and emission filters can be conveniently combined in a fluorescence filter cube holder and placed within the microscope in a standard filter cube turret, but excitation filters must be placed upstream of the dichroic.

For PALM-imaging the activated state of EosFP, the authors use the dichroic FF562-Di02-25 × 36 (Semrock) and the bandpass emission filter FF01-617/73-25 (Semrock). For imaging the inactive state of EosFP or the activated state of Dronpa, the dichroic T495lp (Chroma) and the bandpass emission filter ET525/50 (Chroma) are used; equivalent results can be obtained with a standard GFP filter cube set.

High NA objectives

11 To achieve TIRF, the NA of the objective lens must be greater than the index of refraction n of the sample (typically 1.38 for cellular components). The number of objectives that satisfy this criterion are limited, and practically the investigator is limited to

objectives of NA 1.45, 1.49, and 1.65 (the last manufactured exclusively by Olympus).

Higher NAs imply both better photon collection efficiency and an increased range of angles over which TIRF is achieved (wider TIRF annulus). Better photon collection efficiency results in a greater signal-to-noise ratio and thus higher localization precision of individual molecules. A wider TIRF annulus leads to a greater range of adjustment of the evanescent wave decay length, and makes achieving TIRF easier than with a more limited annulus, as it is easier to focus a spot at the BFP of the objective without clipping the beam. The investigator is thus urged to purchase the objective with the highest possible NA, subject to the constraints discussed below.

It is important to note that the 1.65 NA objective, while providing substantially better TIRF than other objectives, requires expensive high-index (n = 1.78) coverslips (APO100X-CG, Olympus), and high-index (n = 1.78) immersion oil (Series M, Cargille). The oil is toxic to work with, requiring gloves and added safety precautions, and the coverslips are expensive and difficult to reclean. The oil also absorbs in the visible spectrum, particularly at the 405-nm activation wavelength. It thus degrades over time and may need to be replaced during an experiment. Degradation is exacerbated at higher laser powers and elevated temperatures, making this objective unsuitable for experiments on living cells and for the fastest PALM imaging (where increased power is necessary to bleach activated molecules as fast as possible). Obtaining high-quality DIC images with this objective is problematic, as it is not strain-free. Furthermore, it is not a plan objective, so care must be taken to image the specimen near the center of the field-of-view; otherwise aberrations degrade the quality of the point spread function (PSF) and thus limit the localization precision. Despite these caveats, the authors have observed >1.5× photon collection efficiency of the 1.65 NA objective compared to a 1.49 NA objective and significantly lower autofluorescence of the high-index coverslips compared to the more conventional glass coverslips used with the lower NA objective. The authors thus recommend the 1.65 NA objective for

PALM-imaging fixed samples when the PALM image quality is of paramount importance and when acquisition time is not critical. For applications when high-quality DIC is important, on living cells that require 37°C, or when speed is critical, the 1.49 NA objective is the better choice.

When using 1.45 or 1.49 NA objectives, it is important to use the correct immersion oil and coverslip thickness in order to minimize image aberrations (especially spherical aberration). Most high NA oil objectives are designed to work with no. 1.5 thickness glass coverslips; the authors use 25-mm no. 1.5 coverslips from Warner Instruments (cat. no. 64-0715). Index-matched immersion oils can be obtained from Cargille Laboratories—the authors recommend using type DF immersion oil, as it has very low autofluorescence and minimizes aberrations (type FF oil is marginally less autofluorescent, but introduces slight aberrations in the PSF).

EMCCD camera

12 To take full advantage of the wide-field TIRF geometry in PALM and to amplify the single-molecule fluorescence emissions from PA-FPs, use an electron-multiplying cooled CCD (EMCCD) camera as the detector.

These cameras are capable of single-photon detection, as they employ an on-chip multiplication gain that boosts weak signals above the readout noise of the camera. Furthermore, fast (up to 10 MHz/pixel) readout and the ability to operate the camera in frame-transfer mode (spooling acquired data to disk while simultaneously acquiring new data) allow rapid PALM-imaging. The ability to cool the chip to −50°C or less ensures that dark noise (thermal motion of charges in the sensor that can be spuriously counted as photons) is negligible. Most chips can also be purchased with a back-illuminated option (light impinges on the back side of a thinned CCD instead of the front side), leading to a quantum efficiency (the ratio of incident to detected photons) of ~90% across the visible spectrum.

Many single-molecule fluorescence laboratories use EMCCD cameras from Andor Technology. Several options exist, with different pixel sizes, chip sizes, and

readout speeds. The investigator should consider the total system magnification (important in optimizing localization accuracy, discussed below) and desired imaging area before deciding what chip to purchase.

The authors use a DV887ECS-BV (Andor Technology) as the EMCCD, operating in frame-transfer mode and with 10 MHz A/D readout speed. A 512 × 512 pixel chip with 16-μm pixels and a system magnification of 120 offers a total field-of-view of ~70 μm. In practice, a smaller region of the chip is used for imaging (typically 128 × 128 or 256 × 256 pixels) for decreased acquisition time and decreased file sizes.

Optimizing system magnification

13 When localizing single molecules, it is important to match the pixel size of the EMCCD camera to the size of the point spread function (PSF, the diffraction-limited image of a point emitter). If the pixel size is too large, the molecule's PSF will be concentrated within too few pixels (undersampled), and there will not be sufficient spatial resolution to determine the center of the PSF precisely. Conversely, if the pixel size is too small, the PSF will be spread out across too many pixels, and the signal/noise per pixel will be too low to precisely determine the PSF center. The best choice is a pixel size that is approximately equal to the standard deviation in the PSF—see Thompson et al. (2002) for a more complete discussion.

Given the different magnifications of the high NA objectives mentioned above (typically 60× or 100×), it is thus often necessary to increase the total magnification of the imaging system to meet the above criterion. This is accomplished either by the use of internal magnification lenses in the microscope system (usually either a 1.6× or 2× system), or a magnification system placed immediately between the camera and microscope port.

When imaging with the 100×, 1.65 NA objective, the authors employ a 1.2× C-mount adaptor (Diagnostic Instruments, DD12NLC) before the EMCCD for a total system magnification of 120×. When using the 60×, 1.49 NA objective, the authors employ a 2× internal magnification lens and a 1.2× C-mount adaptor for a total magnification of 144×. The effective pixel size when using the camera mentioned above is thus 133 or 111 nm depending on the objective used.

Computer hardware and software requirements

14 A computer with sufficient RAM, processor power, and hard drive space to process and store the stack of single-molecule frames that make up an eventual PALM image is essential. Additionally, the computer must have a slot for a digital acquisition card—the Andor EMCCD cameras typically come with their own card (PCI format). Minimum requirements for running the Andor EMCCD are a 2.4 GHz Pentium processor, 1 GB of RAM, and Microsoft Windows 2000 or XP. An analog output board and/or USB interface may be useful for controlling the power of activation and excitation lasers.

> *The authors use an industrial computer (Advantech) with 2 GB RAM, a dual-core 3 GHz processor, and a 320 GB hard drive. As PALM images are typically composed of tens of thousands of single-molecule frames (corresponding file sizes can easily be >5 GB, especially if large fields of view are imaged), large hard drives are necessary for initial storage of data—the authors thus recommend purchasing as large a hard drive as possible. For long-term storage of PALM data, a server with larger storage capacity is recommended. A fast connection to archival storage is also helpful, to prevent long delays while transferring data.*

15 As PALM imaging is expedited by simultaneously activating the PA-FPs and exciting them, in principle no sophisticated software is needed to independently control or shutter the lasers. The Andor EMCCD cameras come with software [Andor Solis (i)] that is sufficient for acquiring PALM single-molecule image stacks, but in practice it may be desirable to develop integrated software that allows the user to control the laser power (via analog or TTL control), camera acquisition parameters (EM gain, exposure time, and total number of recorded frames), and shuttering for the lasers.

16 As recording a long series of single-molecule frames can be relatively taxing on a computer, the authors perform the localization analysis and image rendering post acquisition using a different computer and appropriate analysis software. With efficient coding, it may be possible to perform the analysis in real-time, or close to real-time, thus eliminating the need for transporting large data files to a different analysis computer. The basic strategy in rendering PALM images is to replot each molecule m as a Gaussian centered at coordinates $\mathbf{x}_m$, $\mathbf{y}_m$ and of width $\boldsymbol{\sigma}_m$ (the latter represents the positional uncertainty, or

standard error on the mean position of the molecule), where σ_m is typically much less than the positional standard deviation in the original diffraction-limited PSF, s_m. The relevant analysis can be broken down into several steps. First, intensity peaks in the raw data that correspond to individual molecules (or fiducial markers, see Basic Protocol 2 below) are identified. This identification allows image data corresponding to a molecule to be summed across all frames and pixels in which the molecule appears. Second, x_m, y_m, and σ_m are determined by fitting the summed intensity data to a Gaussian mask, according to the theory described in Thompson et al. (2002). If fiducial markers are used in the experiment, these parameters can be corrected for sample drift during the acquisition. Finally, the molecules are rendered as Gaussians whose brightness indicates the probability that the molecule can be found at a given location. A more complete description of the analysis software is beyond the scope of this unit, but the reader is directed to the supplementary information in Betzig et al. (2006) for more detailed information. Numerous free software packages for PALM data processing and rendering are now available on the World Wide Web: two examples are QuickPALM (http://code.google.com/p/quickpalm/) and rapidSTORM (http://www.super-resolution.biozentrum.uni-wuerzburg.de/home/rapidstorm/).

PALM-IMAGING tdEos/PAXILLIN DISTRIBUTIONS IN FIXED CELLS

This protocol describes the PALM imaging of tdEos/paxillin distributions in fixed fibroblast cells. The protocol can be broken up into several steps. First, the cells must be transiently transfected with the tdEos/paxillin plasmid and plated onto appropriately cleaned coverslips. Although the cells can be transfected with common chemical reagents—e.g., Lipofectamine (Invitrogen), Effectene (Qiagen), FuGENE (Roche)—the authors have had far better success with the Nucleofection kit from Amaxa Biosystems, routinely achieving transfection efficiencies of >70% with high cell viability. Cleaning coverslips, plating cells, and subsequent transfection are covered in Support Protocols 1 and 2. Second, the transfected cells must be chemically fixed under conditions that preserve as much of the native cellular structure and EosFP fluorescence as possible. The fixation procedure described below is a modification of the protocol described in Galbraith et al. (1998). Finally, the fixed, transfected cells are PALM-imaged with a microscope similar to that described in Basic Protocol 1.

Although the example described here is the imaging of tdEos/paxillin in HFF-1 cells, the protocol is general: the authors have successfully adapted it for PALM-imaging vinculin, actin, α-actinin, and zyxin in CHO and NIH 3T3 cells.

Materials

EM grade paraformaldehyde

Clean water (filtered through a Millipore system)

10 N NaOH solution

2 × PHEM buffer (see recipe)

Cleaned coverslips (Support Protocol 1) plated with HFF-1 cells transfected with tdEos/paxillin, in 35-mm plastic dishes (Support Protocol 2)

Immersion oil

100-nm and 40-nm Au particles (Microspheres-Nanospheres, cat. nos. 790114-010 and 790122-010)

Chemical hood

1-liter glass beaker

Hotplate with magnetic stirring capability

Magnetic stir bar

0.2-μm filter

37°C warm room or equivalent heating system

Fine steel forceps

Microscope set up (as described in Basic Protocol 1)

Lens paper

EMCCD camera (see Basic Protocol 1)

Benchtop vortexer/sonicator

Fix transfected cells

1 Prepare 4% paraformaldehyde (PF) solution by adding 4 g PF to 100 ml clean water in a glass beaker. Place the beaker (with a magnetic stir bar) on a hotplate, and heat the solution to ~80°C while stirring. Carefully add 80 μl of 10 N NaOH (this is necessary to fully dissolve the PF) to the mixture. When the PF appears dissolved, filter the solution using a 0.2-μm filter to remove any residual solid particulates.

> *The investigator should wear gloves, and this procedure should be conducted in a fume hood, as paraformaldehyde is quite toxic. Monitor the solution carefully, as it should be kept from boiling.*

2 Prepare 2% (v/v) PF/1 × PHEM buffer (fixative) by combining the 4% PF and 2 × PHEM solutions in equal volumes. Also prepare 1 × PHEM by combining 2 × PHEM and clean water in equal volumes. Heat the fixative and 1 × PHEM to 37°C.

Fresh fixative should be prepared daily for best morphological preservation of the cells.

3 Transfer the 35-mm dish containing the transfected sample (Support Protocol 2) from the incubator to the warm room. Gently pipet the growth medium off the cells and replace it with 1 ml prewarmed fixative. Incubate for 15 min at 37°C, then wash the coverslips three times, each time with 1 ml 1 × PHEM.

Pipetting/removing solutions should be done gently to ensure that cells are not ripped from the coverslip. Care should be also taken to ensure that the coverslip is completely immersed in liquid, so that it does not dry out.

Identify transfected cells that are suitable for PALM

4 With forceps, carefully lift and transfer the fixed sample from the 35-mm plastic dish to the sample holder and microscope stage. Immerse the sample in 1 × PHEM once the sample is placed in its holder (to prevent it from drying out) and wipe off the bottom surface of the coverslip (the side that will face the objective) with lens paper (it is essential that water and immersion oil do not mix during the imaging).

5 Apply the appropriate immersion oil to the chosen TIRF objective.

6 Focus on the cells with the microscope eyepiece, using either brightfield or DIC optics.

7 Start the acquisition software and cool the EMCCD camera to −50°C or lower.

The authors have not noticed a significant decrease in dark noise below −50°C.

8 At the maximum gain of the EMCCD, use the 488-nm laser at low power in combination with the GFP filter cube to scan the sample in TIRF and identify cells that express tdEos/paxillin fusion proteins. If a stage with linear encoders is used, note the positions of suitable cells so that they can be easily found later.

As paxillin forms distinctive finger-like structures at the cell surface, identification of transfected cells should be straightforward.

Note that because EosFP switches its fluorescence from green to orange upon photoactivation, the green fluorescence (excited by 488-nm light) provides a convenient monitor of protein expression at the diffraction-limited level, and can be used to screen cells to decide if they are suitably transfected for PALM.

The determination of the 488-nm power to use in this step is empirical and depends on the particular experimental configuration. Generally, the authors use as low a power as possible in illuminating the sample (10 to 30 μW over an excitation region ~30 μm in diameter, for intensities of ~1 W/cm^2 at the sample) so as not to bleach the inactive EosFP molecules before PALM-imaging. A power meter is useful for measuring the laser power; the authors use a FieldMaxII-TO digital power meter (Coherent).

With experience, the investigator can use the real-time intensities displayed by the camera acquisition software to determine what an acceptable level of transfection is, how much power to apply, and what exposure time should be used for minimal bleaching of the sample. Finally, note that there is often an inverse correlation between the cell health and the level of transfection; brightly fluorescent cells may not necessarily have the best morphology and vice versa. The investigator should find a cell that is sufficiently transfected but also appears to have good morphology in DIC.

9 If a suitable cell is found, prepare a 10× dilution of Au particles in 1 × PHEM. Vortex the suspension until it is well-mixed (it may be necessary to also vortex the stock solution of fiducials if they have settled to the bottom of the container).

Sonicating the mixture can also aid in breaking up Au aggregates.

Because the Au particles are fluorescent but do not bleach during the acquisition period, they function as fiducial markers, and are important in correcting for mechanical drift during the acquisition period (Betzig et al., 2006). The basic strategy is to determine the position of the fiducials over the entire image acquisition, and to subtract these positions from the

coordinates of the localized molecules when reconstructing a PALM image.

The authors have found that 100-nm Au particles are best when imaging the orange, activated state of EosFP, whereas 40-nm Au particles are better when imaging the green, activated state of Dronpa.

The concentration of Au fiducials (and incubation time) should be determined empirically. Generally it is best to have 2 to 5 fiducials visible in the imaging field of view when PALM-imaging—their positions can be averaged and used to remove drift more accurately than if only one fiducial is found. Conversely, too many fiducials impede the isolation of single molecules, as it is difficult to identify molecules located near a fiducial.

10 Carefully pipet off the 1 × PHEM solution covering the coverslip, and replace it with 1 ml of the Au suspension. Incubate 5 to 10 min, or long enough for the Au particles to settle and stick to the coverslip surface, at 25°C.

11 Once a suitable density of Au fiducials is achieved, rinse the sample once with 1 ml 1 × PHEM.

PALM-image a suitable cell

12 Switch to the appropriate filter cube for imaging the activated state of EosFP, and illuminate the sample with the 561-nm laser. Adjust the laser power until it is sufficient for achieving good signal-to-noise (S/N) images of single activated molecules and fiducials at the desired exposure time.

The laser power should be increased until single molecules can be visualized at high S/N at a minimal exposure time. The intensity of fiducials should be comparable to single-molecule fluorescence; occasionally, it is possible that fiducials will be too dim or too bright (the latter will saturate the EMCCD, and are usually indicative of Au aggregates), in which case the investigator is advised to add more fiducials. Also, in the case of the 1.65 NA objective, a practical limit on the maximum laser power is set by the absorption in the immersion oil. The final power and exposure time are dependent on the details of the investigator's setup, and are again best determined empirically. The authors typically use ~10 mW of 561-nm power (over an

excitation region 30 μm in diameter, for intensities of ~ 1 kW/cm^2) and 20 to 50 msec exposure times.

13 With the laser power and exposure time adjusted, start the PALM acquisition. Illuminate the sample initially only with the 561-nm laser beam, to bleach the small population of EosFP molecules that appears fluorescent at the start of the acquisition.

There is a population of EosFP that is spontaneously activated (and is thus excited) at the start of any PALM acquisition. These molecules must be bleached before activating further molecules, otherwise too many molecules will be activated at once, impeding the isolation of individual molecules and degrading the localization precision (Fig. 4.21.8A).

14 Illuminate the sample with the 405-nm activation laser at low power (it may be necessary to insert neutral density filters into the beam path to reduce the laser power). As the acquisition proceeds and the pool of unactivated molecules is depleted, increase the activation power in order to keep the number of activated molecules roughly constant per frame.

Care must be taken to ensure that the optimal number of molecules is activated per frame. If too few molecules are activated at a given time, the data acquisition is slowed down and it will take longer to acquire the complete PALM dataset (Fig. 4.21.8B). The 405-nm laser power should be increased until the molecular density per frame increases.

If too many molecules are activated, the image will appear diffraction-limited, retarding localization accuracy (Fig. 4.21.8A). The 405-nm laser power should be decreased until single molecules are easily discerned. From a speed perspective, the optimal activation power occurs when molecules appear "bumper to bumper," separated just enough to be spatially resolved (Fig. 4.21.8C).

15 Proceed with data acquisition, collecting frames until the population of single activated molecules becomes insignificant even at high activation laser power.

For long acquisitions, and depending on the mechanical stability of the instrument, it may be necessary to manually adjust the focus of the objective during PALM-imaging. Although several commercial auto-focus systems exist for correcting objective focus

drift during data acquisition, there is always a slight time lag between when the auto-focus system is engaged and when the focus is reset to the original position. A simpler (and less expensive) alternative is to manually adjust the focus of the microscope during the PALM acquisition. A microscope system with an ultra-fine focus is useful for this purpose.

DUAL-COLOR PALM-IMAGING OF tdEos/VINCULIN AND DRONPA α-ACTININ IN FIXED CELLS

Single-color PALM can reveal the spatial distribution of a target protein at >10× resolution than with conventional fluorescence microscopy. While informative, cellular function is often driven by the interaction of two or more proteins. It would thus be valuable to accurately determine the spatial distribution of several interacting proteins using a multicolor superresolution technique. As described in Shroff et al. (2007), it is possible to serially PALM-image two adhesion complex proteins by tagging the first with EosFP and the second with Dronpa. This protocol shows that, with relatively few modifications, it is possible to adapt Basic Protocol 2 for the PALM-imaging of vinculin (Ziegler et al., 2006) and α-actinin (Otey and Carpen, 2004; Fig. 4.21.9).

Materials

HFF-1 cells cotransfected with tdEos/vinculin and Dronpa/α-actinin plasmid constructs (these plasmids are made in-house by the authors, but can also be obtained from Mike Davidson, Florida State University)

100-nm and 40-nm Au particles (Microspheres-Nanospheres, cat. nos. 790114-010 and 790122-010)

Additional reagents and equipment for cleaning coverslips (Support Protocol 1), transfecting cells (Support Protocol 2), and PALM-imaging both Eos (Basic Protocol 2) and Dronpa

Prepare sample

1 Follow Support Protocols 1 and 2 for cleaning coverslips and transfecting cells. Instead of using the Amaxa system to nucleofect cells with only a single plasmid, cotransfect cells with both plasmid constructs.

As transiently transfecting cells with more than one expression plasmid stresses the cellular machinery more than if a single plasmid is transfected, some optimization of DNA concentration may be necessary to obtain optimal cell viability and expression level. The investigator is recommended to start with equal

concentrations of both plasmid DNAs, and increase/decrease the concentration of either or both until a high percentage of cells survive the nucleofection and express enough of both proteins for good dual-color PALM-imaging.

2 Follow steps 4 to 8 in Basic Protocol 2 to identify transfected cells suitable for PALM.

As α-actinin cross-links actin stress fibers, and vinculin localizes to adhesion complexes at the termini of stress fibers, cells that are doubly-transfected should exhibit both morphologies (compare Fig. 4.21.9A and Fig. 4.21.9B). It should thus be possible to identify appropriately transfected cells by scanning the sample in TIRF, using the 488-nm laser.

3 Prepare a 1:1 mixture of 40 nm Au particles and 100 nm Au particles, and incubate the sample with a 10× dilution as described in steps 9 to 11 of Basic Protocol 2.

As both Eos and Dronpa are to be imaged, it is useful to include both kinds of fiducials. For registering both Eos and Dronpa images post-acquisition, it is essential that some fiducials show up in both Eos and Dronpa channels.

PALM-image the Eos channel

4 Follow steps 12 to 15 in Basic Protocol 2 to PALM-image the Eos channel. Ensure that all Eos molecules are bleached before proceeding.

As the technique described in Shroff et al. (2007) is serial, it is important to thoroughly activate and bleach the tdEos/vinculin molecules before attempting to PALM-image the Dronpa/α-actinin. Otherwise, residual Eos molecules that fluoresce in the green channel will be incorrectly identified as Dronpa molecules. The authors recommend doing control experiments akin to those described in Figure 4.21.10, to gain an idea of what the background should look like in the Eos channel after all Eos molecules are bleached, and before PALM-imaging the Dronpa channel. Such crosstalk control experiments are also a good check to ensure that fluorescence emission filters are optimized and that bleed-through of one fluorescent tag onto the other channel is negligible.

PALM-image the Dronpa channel

5 Turn off the 405-nm and 561-nm lasers. Switch to the GFP filter cube for imaging Dronpa. Start the acquisition software and illuminate the sample with the 488-nm laser.

Initially, the pool of Dronpa molecules that were activated during the course of PALM-imaging Eos will fluoresce, contributing a bright green background and making it difficult to discern single Dronpa molecules. Within several hundred frames (depending on the exposure time and laser power used), this background should die down, as Dronpa molecules are driven into a dark state with prolonged exposure to 488 nm. Ensure that the imaging area appears mostly dark (there are always some Dronpa molecules that are spontaneously active and appear to blink during the acquisition) before proceeding to the next step.

The high-index immersion oil used with the 1.65 NA objective is considerably less tolerant to 488 nm than 561 nm, as the absorption is greater in the bluer portion of the spectrum. Consequently, it is recommended to use a lower laser power with 488 nm than with 561 nm. The choice of how much power to use is best determined by the investigator. The authors use 3 to 5 mW (measured prior to the entrance of the objective) and 50 to 100 msec exposure time.

6 After the bright background of activated Dronpa molecules dies down, turn on the 405-nm laser at lower power. Follow steps 14 and 15 of Basic Protocol 2, gradually ramping the 405-nm laser power until all Dronpa molecules have been activated and bleached.

PREPARING CLEAN COVERSLIPS

For PALM experiments, the coverslips upon which the cells are grown should be cleaned as thoroughly as possible. This is because debris deposited on the coverslips is often excited by the activation and excitation lasers, and will contribute either to elevated background counts in each frame or as spurious single-molecule fluorescence. This protocol describes a chemical cleaning method based on the industry standard for removing contaminants from semiconductor wafers. It is considerably less reactive (and hazardous) than other cleaning methods, but still adequate for PALM-imaging. Although 1% hydrofluoric acid (HF) is suitable for cleaning conventional glass coverslips in ~5 min (see supporting information in Betzig et al., 2006), it reacts with the high-index coverslips used with the 1.65 NA objective, rendering them opaque and unsuitable for imaging.

Materials

Ammonium hydroxide

Hydrogen peroxide

Clean water (filtered through a Millipore system)

Methanol (spectroscopic grade)

Clean air supply (preferably filtered through a 0.2-μm pore-size filter)

RBS-35 liquid detergent concentrate (Pierce, cat. no. 27950)

Acetone (spectroscopic grade)

Chemical fume hood

100-ml graduated cylinder

250-ml glass beaker

25-mm diameter glass coverslips, no. 1.5 (Warner Instruments, cat. no. 64-0715; for use with 1.45 NA or 1.49 NA objectives)

High-index 20-mm diameter coverslips (Olympus, cat. no. APO100X-CG; for use with 1.65 NA objective)

Hotplate with magnetic stirring capability

Magnetic stir bar

Corrosion-resistant staining rack for holding coverslips (Thomas Scientific, cat. no. 8542E40)

Metal tongs for holding staining rack

Fine steel forceps

Compressed butane/natural gas, burner, and lighter

1 In a chemical fume hood, use a 100-ml graduated cylinder to prepare the etch solution by combining 125 ml clean water, 25 ml ammonium hydroxide, and 25 ml hydrogen peroxide in a 250-ml beaker. Heat the mixture to 80°C, and add a bar for stirring.

> *The investigator should wear gloves, and take care to avoid exposing the skin to the corrosive solvents used in the cleaning solution.*

2 Load the staining rack with coverslips and place it into the etch solution with the metal tongs. Let the coverslips incubate at least 3 hr (overnight is preferred for high-index coverslips) while stirring.

3 Fill another 250-ml beaker with clean water and carefully transfer the rack into the new beaker. Rinse the rack with copious amounts of clean water (at least 10 beaker volumes). Dispose of the cleaning solution appropriately.

4 Carefully remove a cleaned coverslip from the rack with the steel forceps (holding the coverslip near the edge) and rinse both sides with methanol.

The methanol can be conveniently stored in a squeeze bottle and squirted onto the coverslip.

5 Rapidly remove excess methanol from the coverslip by blowing it away with the filtered air.

A pipet tip can be connected with tubing to the air supply and used as an aid in blowing away the methanol.

6 Connect the burner to the butane (or natural gas), and light. Pass the coverslip quickly through the topmost portion of the flame, and repeat this process three times.

The coverslip should be dry (or almost).

Care must be taken not to hold the coverslip too long (more than a second) in the flame, otherwise it may crack due to thermal shock.

7 Store the cleaned coverslip dry in a clean staining rack. Repeat steps 4 to 6 with the rest of the coverslips. Cover the filled staining rack to prevent dust from settling on the coverslips, and store dry until the coverslips are ready for use.

8 The high-index coverslips are expensive, but can be recleaned and reused several times. Store used coverslips in a 2% solution of RBS detergent solution, and rinse with copious amounts of clean water before repeating steps 1 to 4. Before repeating steps 5 to 7, sonicate the coverslip for 5 min in acetone and rinse well with clean water.

TRANSFECTION OF tdEos/PAXILLIN INTO HFF-1 CELLS

Using the Nucleofector 96-well shuttle system (Amaxa Biosystems), HFF-1 cells are nucleofected with plasmid DNA in accordance to the manufacturer's guidelines for optimal viability and transfection efficiency. Nucleofection of lower passage cells harvested while in log growth, with highly purified DNA, results in transfection efficiencies > 70%.

NOTE: All solutions and materials coming into direct contact with live cells must be sterile and proper aseptic technique should be used accordingly.

NOTE: All incubations are performed in a humidified 37°C, 5% CO_2 tissue culture incubator unless otherwise specified.

Materials

70% ethanol

Human plasma fibronectin diluted in 1 × PBS (without divalent cations)

1% (w/v) BSA/DMEM HG, heat-inactivated (see recipe)

HFF-1 growth medium (see recipe)

0.05% (w/v) trypsin-0.53mM EDTA

Cell Line 96-well Nucleofector Kit SE (Amaxa, VHCA-1001) containing:

SE solution

Supplement

Plasmid: tdEos/paxillin (~0.5 to 1 μg/μl)

Normal human foreskin fibroblast (HFF-1) cells (ATCC cat. no. SCRC-1041) grown in 75-cm^2 cell culture flasks with 0.2-μm vent caps for 2 to 3 days before transfection

Compressed butane/natural gas, burner, and lighter

Fine steel forceps

Cleaned coverslips (see Support Protocol 1)

35 × 10–mm cell culture dishes

37°C water bath

1.5-ml microcentrifuge tube *or* 15-ml conical centrifuge tubes

Centrifuge capable of 90 × *g* (Eppendorf 5810 or equivalent)

Centrifuge rotor (Eppendorf 5810 A-4-62 or equivalent)

Rainin LTS pipets (0.1 to 200 μl)

Rainin LTS tips (RT-L10F and RT-L200F)

Nucleofector 96-well shuttle system (Amaxa Biosystems)

Additional reagents and equipment for performing a viable cell count (*UNIT 1.1*)

Pre-coat coverslips with 10 μg/ml fibronectin (day 1)

1 Spray forceps with 70% ethanol and pass through flame of ignited butane gas to sterilize. Use forceps to transfer each cover slip to a 35 × 10–mm dish. Add ~200 μl of 10 μg/ml

fibronectin-1× PBS solution to coverslip surface and store overnight at 4°C.

Transfect cells (day 2)

2 Remove fibronectin solution and block coverslips with 200 µl heat-inactivated 1% BSA-DMEM. Store 1 to 2 hr at room temperature.

3 Remove BSA solution and add 1.5 to 2.0 ml HFF-1 growth medium per dish; incubate 30 to 60 min at 37°C in humidified 5% CO_2 to equilibrate dishes to culture conditions prior to plating cells.

4 Prewarm the HFF-1 growth medium and trypsin-EDTA in a 37°C water bath.

5 Acclimate the Amaxa Nucleofector Kit SE and plasmid to room temperature.

6 Mix the volume of Nucleofector SE solution required by experiment. Use a mix ratio of 162.5 µl SE solution to 36 µl 96-well supplement. A total of 20 µl is required per shuttle well.

7 Use 5.0 ml trypsin-EDTA to detach HFF-1 cells per 75-cm^2 tissue culture flask. Neutralize cell suspension with an equal volume of HFF-1 growth medium.

Before harvest, cells should be ~70% confluent.

8 Count an aliquot of the cells (*UNIT 1.1*) and calculate the volume sufficient to nucleofect 4 to 5 × 10^5 live cells per shuttle well. Transfer cell suspension to microcentrifuge tube(s) and centrifuge 7 min at 90 × *g*, room temperature.

If a larger volume of cell suspension is required, a larger 15- ml conical centrifuge tube may be used to centrifuge cells.

Per manufacturer's recommendation, one spin-down is preferred.

9 Carefully, remove all fluid from the pellet and gently resuspend the cells in 20 µl Nucleofector SE solution (prepared in step 6) per 4 to 5 × 10^5 live cells. Add ~1 µg plasmid DNA per 20 µl of Nucleofector SE solution. Gently mix cells, plasmid, and nucleofector solution. Load 20 µl per shuttle well.

Per manufacturer recommendation, the volume of plasmid solution should not exceed 2 µl per shuttle well.

Rainin RT-L10F tips are recommended by manufacturer for loading shuttle wells. Avoid creating air bubbles.

10 Load plate in Amaxa apparatus, select program DS 137, and initiate nucleofection.

11 Upon completion of nucleofection, remove shuttle plate and add 80 µl HFF-1 growth medium (from dishes prepared in step 3) per shuttle well. Place shuttle plate inside incubator. After 10 min, transfer contents of each shuttle well to a pre-equilibrated 35-mm dish (prepared in step 3) and gently dispense cell suspension on top of coverslip surface.

12 Incubate plates at 37°C in 5% humidified CO_2.

Cells are imaged ~24 to 36 hr post-nucleofection.

REAGENTS AND SOLUTIONS

*Use ultrapure water purified by reverse osmosis and Millipore Milli-Q system in all recipes and protocol steps. For common stock solutions, see **APPENDIX 2A**; for suppliers, see **SUPPLIERS APPENDIX**.*

BSA, 1% (w/v)/DMEM HG (heat-inactivated)

Prepare 1% (w/v) BSA fraction V (EMD OmniPur 2930) in high glucose DMEM (DMEM HG) without phenol red (Cellgro, 17-205-CV) supplemented with 4 mM L-glutamine. Heat for 30 min at 56°C and filter with a 0.2-µm cellulose acetate filter. Store up to 1 month at 4°C.

HFF-1 growth medium

High glucose DMEM without phenol red (Cellgro, 17-205-CV)

15% (v/v) FBS

4 mM L-glutamine

Store up to 1 month at 4°C

PHEM buffer, 1 ×

60 mM PIPES

25 mM HEPES

10 mM EGTA

2 mM $MgCl_2$

Adjust pH to 6.9 using NaOH

Store up to 1 year at 4°C

COMMENTARY

Background Information

Resolution considerations in PALM—The ultimate resolution achievable in PALM (Betzig et al., 2006), stochastic optical reconstruction microscopy (STORM; Rust et al., 2006), and fPALM (Hess et al., 2006) is dependent on two criteria: the localization precision (how well the center of each PSF can be determined) and the density of available photoactivatable molecules.

In the case of negligible background, it can be shown (Thompson et al., 2002) that the error in the PSF center determination is inversely proportional to the square root of the number of collected photons. Thus, a photoactivatable tag that emits 100-fold more photons than another would give a 10-fold increase in localization precision. Indeed, synthetic fluorophores such as Cy3 yield $>10^6$ collected photons and enable localization down to ~1.5 nm (Yildiz et al., 2003) in ideal conditions. Maximizing the collection efficiency of the instrument (with high NA objectives and appropriate filters and camera) while rejecting background (with TIRF) is thus critical for high localization precision.

Although a high number of collected photons are desirable from a localization standpoint, in practice other factors (errors in the PSF fit, drift correction, background due to other fluorescent tags present at high density, or autofluorescence of the sample) limit the localization precision to ~10 nm for the majority of photoactivatable molecules. Furthermore, from the perspective of PALM-imaging as fast as possible, it is undesirable to use a tag that emits too many photons, as it takes a longer time to bleach the tag. Molecular bleaching is in fact the rate-limiting step in acquiring more data, as a given tag should be bleached before another can be activated and imaged in the same diffraction-limited region (DLR).

EosFP is well-matched to PALM needs: using the 1.65 NA objective and TIRF, >1000 photons are collected on average per molecule. This is enough photons to localize most molecules to within 20 nm (>85% of the molecules in Figure 4.21.1 are localized to within this precision), but not so many photons that molecules persist over too many frames. In contrast, Dronpa emits too few photons per switching cycle, and the localization precision and thus resolution are compromised as a result [compare Dronpa and Eos images in Shroff et al. (2007)].

Besides localization precision, the other key determinant of resolution is the density of molecules. According to the Nyquist-Shannon sampling theorem (Shannon, 1949), the sampling interval (mean distance between neighboring localized molecules) must be at least twice as fine as the desired resolution; otherwise, the feature of interest will be under-sampled and unresolved. For example, in two dimensions (applicable for PALM-imaging adhesion complex systems), to achieve 10-nm resolution, molecules must be spaced 5 nm apart in each dimension, for a minimum density of 4×10^4 molecules/μm^2 or ~2000 molecules in a DLR of 250-nm in diameter.

As mentioned in the introduction, PA-FPs are better suited to achieving these densities than caged dye conjugated antibodies, as although caged dyes are often smaller than PAFPs, the large size of antibodies still limits the densities that can be practically achieved. This situation may change if small-molecule labeling strategies (Chen and Ting, 2005; Giepmans et al., 2006) improve to the point where caged dyes can be routinely attached to a target protein with very high specificity.

Regardless of the labeling strategy (endogenous PA-FPs, exogenous caged dyes, or the cyanine dyes used in STORM), another factor that influences both the maximum achievable density and the localization precision is the contrast ratio, which is the ratio in fluorescence intensity between the inactive and activated states of the photoswitchable molecule. If the contrast ratio is less than the density of the probe in a given diffraction-limited region, the weak intensity from the inactive molecules will overwhelm the intensity from a single activated molecule, confounding both localization and the measurement of densely labeled samples. Figure 4.21.2 illustrates the contrast ratio for four common PA-FPs, showing that the large contrast ratio of Eos, which has been shown to be capable of measuring densities as high as 10^5 molecules/μm^2 (Betzig et al., 2006), or sufficient for 10-nm resolution, results in superior images, both at the single-molecule and PALM levels. The contrast ratio has not been measured for most photoswitchable molecules, but based on the reports so far, EosFP is the only PA-FP able to achieve imaging resolutions <20 nm. Note that the synthetic caged dye Q-rhodamine has a very high contrast ratio (see supporting material in Betzig et al., 2006), and that a new rhodamine-amide with very high contrast ratio has been recently reported (Fölling et al., 2007).

Critical Parameters and Troubleshooting

Although increasing the density of expressed PA-FPs is desirable from the standpoint of the Nyquist criterion and to increase spatial resolution, the investigator should be wary of overexpression artifacts. In some cases, the size of the PA-FP tag may affect the function of the target protein deleteriously. Controls should be done to ensure that the morphological and kinetic characteristics (shape, growth, and motility) of the transfected cells used for PALM-imaging are as close as possible to their untransfected neighbors. As mentioned in Strategic Planning, expressing non-monomeric PA-FPs at high density may also lead to increased aggregation, so the investigator is urged to interpret all PALM results with care.

Transfected cells should be imaged as soon as possible after fixation. The authors have noticed a pronounced decrease in sample fluorescence several hours post-fixation, presumably due to degradation of the PA-FPs. As a decreased number of detected molecules leads to a decrease in the final resolution, the authors fix samples immediately prior to imaging. Also, morphology of the cells is better preserved if fresh fixative is made daily.

During the acquisition period, the most critical parameter to control is the degree of photoactivation at the sample. If too many molecules are photoactivated simultaneously (Fig. 4.21.8A), it will be difficult to localize each one precisely, leading to decreased resolution in the final PALM image. This problem is easy to diagnose by carefully monitoring the acquisition as it proceeds: if the sample is diffraction-limited in appearance, and the investigator cannot make out the blinking and bleaching that is characteristic of single-

molecule fluorescence, the activation power is likely too high and needs to be reduced until single-molecule fluorescence is visible (Fig. 4.21.8C). The authors avoid this problem by starting each PALM acquisition with the activation laser off; only after most molecules are bleached is the activation laser turned on, and at a very low power.

Another important consideration that has been neglected in several recent reports is the importance of the drift correction procedure. Uncorrected drift manifests itself as a blur in the final PALM image. Especially for longer acquisitions, and depending on the mechanical stability of the system, mechanical drift can be >100 nm. It is thus critical to measure and then correct the drift if the desired spatial resolution is to be better than this.

Both the degree of photoactivation and drift correction are important when performing dual-color PALM, but now the investigator must also ensure that the population of Eos-tagged molecules are completely bleached before PALM-imaging the Dronpa channel, or else the Eos molecules will be spuriously identified as Dronpa molecules. As illustrated in Figure 4.21.10, after bleaching out the Eos channel, the level of background counts in the Dronpa channel should be comparable to the background measured in an untransfected cell.

Anticipated Results

When a TIRF microscope is adapted for PALM as described in Basic Protocol 1, EosFP is used as the photoactivatable tag, and the guidelines in Basic Protocol 2 followed, the investigator can expect PALM images similar to Figure 4.21.1, with high (~20 nm) spatial resolution. Following Basic Protocol 3 leads to dual-color superresolution imaging of adhesion complexes, and images akin to Figure 4.21.9. If laser power is not limiting, single-color PALM experiments on living systems are feasible, because molecules can be activated and bleached fast enough to track slowly evolving processes (e.g., adhesion complex dynamics that evolve on the timescale of tens of seconds) at superresolution (Shroff et al., 2008). Dual-color, superresolution imaging of live cells awaits the development of new, spectrally distinct PA-FPs; because the approach outlined in Basic Protocol 3 is serial, it cannot be used in simultaneous two-color imaging. The authors expect that, in time, PALM will yield new biological insights, especially for those systems that can be densely labeled.

Time Considerations

Clean coverslips are prepared in ~12 hr (Support Protocol 1). It takes an additional 12 hr to coat the cleaned coverslips with fibronectin. Once cells are ready for transfection (see Support Protocol 2), it takes ~1 hr to perform the Amaxa transfection and then a further 24 to 48 hr before expression levels are suitable for PALM. Imaging takes between 5 to 30 min if high laser powers are used to bleach the activated molecules, although this time depends on the size of the desired field of view, and the density and number of expressed PA-FPs. Sample preparation thus constitutes the bulk of the preparation time in PALM.

Acknowledgments

The authors thank Jim and Cathy Galbraith (National Institutes of Health) and Na Ji and Tim Brown (Janelia Farm Research Campus) for their feedback and helpful suggestions on the manuscript.

Literature Cited

Ando R, Hama H, Yamamoto-Hino M, Mizuno H, Miyawaki A. An optical marker based on the UV-induced green-to-red photo-conversion of a fluorescent protein. Proc. Natl. Acad. Sci. U.S.A. 2002; 99:12651–12656. [PubMed: 12271129]

Ando R, Mizuno H, Miyawaki A. Regulated fast nucleocytoplasmic shuttling observed by reversible protein highlighting. Science. 2004; 306:1370–1373. [PubMed: 15550670]

Axelrod D. Total internal reflection fluorescence microscopy in cell biology. Traffic. 2001; 2:764–774. [PubMed: 11733042]

Betzig E, Patterson GH, Sougrat R, Lindwasser OW, Olenych S, Bonifacino JS, Davidson MW, Lippincott-Schwartz J, Hess HF. Imaging intracellular fluorescent proteins at nanometer resolution. Science. 2006; 313:1642–1645. [PubMed: 16902090]

Cella Zanacchi F, Lavagnino Z, Perrone Donnorso M, Del Bue A, Furia L, Faretta M, Diaspro A. Live-cell 3D super-resolution imaging in thick biological samples. Nat. Methods. 2011; 8:1047–1049. [PubMed: 21983925]

Chen I, Ting AY. Site-specific labeling of proteins with small molecules in live cells. Curr. Opin. Biotechnol. 2005; 16:35–40. [PubMed: 15722013]

Chudakov DM, Verkhusha VV, Staroverov DB, Souslova EA, Lukyanov S, Lukyanov KA. Photoswitchable cyan fluorescent protein for protein tracking. Nat. Biotechnol. 2004; 22:1435–1439. [PubMed: 15502815]

Chudakov DM, Lukyanov S, Lukyanov KA. Tracking intracellular protein movements using photoswitchable fluorescent proteins PS-CFP2 and Dendra2. Nat. Protocols. 2007; 2:2024–2032. [PubMed: 17703215]

Dempsey GT, Vaughan JC, Chen KH, Bates M, Zhuang X. Evaluation of fluorophores for optimal performance in localization-based super-resolution imaging. Nat. Methods. 2011; 8:1027–1036. [PubMed: 22056676]

Egner A, Geisler C, Middendorff C, Bock H, Wenzel D, Medda R, Andresen M, Stiel AC, Jakobs S, Eggeling C, Schönle A, Hell SW. Fluorescence nanoscopy in whole cells by asynchronous localization of photoswitching emitters. Biophys. J. 2007; 93:3285–3290. [PubMed: 17660318]

Fölling J, Belov V, Kunetsky R, Medda R, Schönle A, Egner A, Eggeling C, Bossi M, Hell SW. Photochromic rhodamines provide nanoscopy with optical sectioning. Angew. Chem. Int. Ed. 46:6266–6270.

Galbraith CG, Skalak R, Chien S. Shear stress induces spatial reorganization of the endothelial cell cytoskeleton. Cell Motil. Cytoskeleton. 1998; 40:317–330. [PubMed: 9712262]

Giepmans BNG, Adams SR, Ellisman MH, Tsien RY. The fluorescent toolbox for assessing protein location and function. Science. 2006; 312:217–224. [PubMed: 16614209]

Gustafsson MGL. Surpassing the lateral resolution limit by a factor of two using structured illumination microscopy. J. Microsc. 2000; 198:82–87. [PubMed: 10810003]

Gustafsson MGL. Nonlinear structured-illumination microscopy: Wide-field fluorescence imaging with theoretically unlimited resolution. Proc. Natl. Acad. Sci. U.S.A. 2005; 102:13081–13086. [PubMed: 16141335]

Heilemann M, van de Linde S, Schüttpelz M, Kasper R, Seefeldt B, Mukherjee A, Tinnefeld P, Sauer M. Subdiffraction-resolution fluorescence imaging with conventional fluorescent probes. Angew. Chem. Int. Ed. 2008; 47:6172–6176.

Hess ST, Girirajan TPK, Mason MD. Ultra-high resolution imaging by fluorescence photoactivation localization microscopy. Biophys. J. 2006; 91:4258–4272. [PubMed: 16980368]

Huang B, Jones SA, Brandenburg B, Zhuang X. Whole-cell 3D STORM reveals interactions between cellular structures with nanometer-scale resolution. Nat. Methods. 2008; 5:1047–1052. [PubMed: 19029906]

Juette MF, Gould TJ, Lessard MD, Mlodzianoski MJ, Nagpure BS, Bennett BT, Hess ST, Bewersdorf J. Three-dimensional sub-100 nm resolution fluorescence microscopy on thick samples. Nat. Methods. 2008; 5:527–529. [PubMed: 18469823]

McKinney SA, Murphy CS, Hazelwood KL, Davidson MW, Looger LL. A bright and photostable photoconvertible fluorescent protein. Nat. Methods. 2009; 6:131–133. [PubMed: 19169260]

Mitchison TJ, Sawin KE, Theriot JA, Gee K, Mallavarapu A. Caged fluorescent probes. Methods Enzymol. 1998; 291:63–78. [PubMed: 9661145]

Otey CA, Carpen O. Alpha-actinin revisited: A fresh look at an old player. Cell Mot. Cytoskel. 2004; 58:104–111.

Patterson GH, Lippincott-Schwartz J. A photoactivatable GFP for selective photolabeling of proteins and cells. Science. 2002; 297:1873–1877. [PubMed: 12228718]

Rust MJ, Bates M, Zhuang X. Sub-diffraction-limit imaging by stochastic optical reconstruction microscopy (STORM). Nat. Methods. 2006; 3:793–796. [PubMed: 16896339]

Shannon CE. Communication in the presence of noise. Proc. IRE. 1949; 37:10–21.

Shroff H, Galbraith CG, Galbraith JA, White H, Gillette J, Olenych S, Davidson MW, Betzig E. Dual-color superresolution imaging of genetically expressed probes within individual adhesion complexes. Proc. Natl. Acad. Sci. U.S.A. 2007; 104:20308–20313. [PubMed: 18077327]

Shroff H, Galbraith CG, Galbraith JA, Betzig E. Live-cell photoactivated localization microscopy of nanoscale adhesion complexes. Nat. Methods. 2008; 5:417–423. [PubMed: 18408726]

Subach FV, Patterson GH, Manley S, Gillette JM, Lippincott-Schwartz J, Verkhusha VV. Photoactivatable mCherry for high-resolution two-color fluorescence microscopy. Nat. Methods. 2009; 6:153–159. [PubMed: 19169259]

Thompson RE, Larson DR, Webb WW. Precise nanometer localization analysis for individual fluorescent probes. Biophys. J. 2002; 82:2775–2783. [PubMed: 11964263]

Tsutsui H, Karasawa S, Shimizu H, Nukina N, Miywaki A. Semi-rational engineering of a coral fluorescent protein into an efficient highlighter. EMBO Rep. 2005; 6:233–238. [PubMed: 15731765]

Weiss S. Fluorescence spectroscopy of single biomolecules. Science. 1999; 283:1676–1683. [PubMed: 10073925]

Wiedenmann J, Nienhaus GU. Live-cell imaging with EosFP and other photoactivatable marker proteins of the GFP family. Expert Rev. Proteomics. 2006; 3:361–374. [PubMed: 16771707]

Wiedenmann J, Ivanchenko S, Oswald F, Schmitt F, Rocker C, Salih A, Spindler K-D, Nienhaus GU. EosFP, a fluorescent marker protein with UV-inducible green-to-red fluorescence conversion. Proc. Natl. Acad. Sci. U.S.A. 2004; 101:15905–15910. [PubMed: 15505211]

Willig KI, Rizzoli SO, Westphal V, Jahn R, Hell SW. STED microscopy reveals that synaptotagmin remains clustered after synaptic vesicle exocytosis. Nature. 2006; 440:935–939. [PubMed: 16612384]

Yildiz A, Forkey JN, McKinney SA, Ha T, Goldman YE, Selvin PR. Myosin V walks hand-over-hand: Single fluorophore imaging with 1.5-nm localization. Science. 2003; 300:2061–2065. [PubMed: 12791999]

York AG, Ghitani A, Vaziri A, Davidson MW, Shroff H. Confined activation and subdiffractive localization enables whole-cell PALM with genetically expressed probes. Nat. Methods. 2011; 8:327–333. [PubMed: 21317909]

Zaidel-Bar R, Itzkovitz S, Ma'ayan A, Iyengar R, Geiger B. Functional atlas of the integrin adhesome. Nat. Cell Biol. 2007; 9:858–867. [PubMed: 17671451]

Zamir E, Geiger B. Molecular complexity and dynamics of cell-matrix adhesions. J. Cell Sci. 2001; 114:3583–3590. [PubMed: 11707510]

Ziegler WH, Liddington RC, Critchley DR. The structure and regulation of vinculin. Trends Cell Biol. 2006; 16:453–460. [PubMed: 16893648]

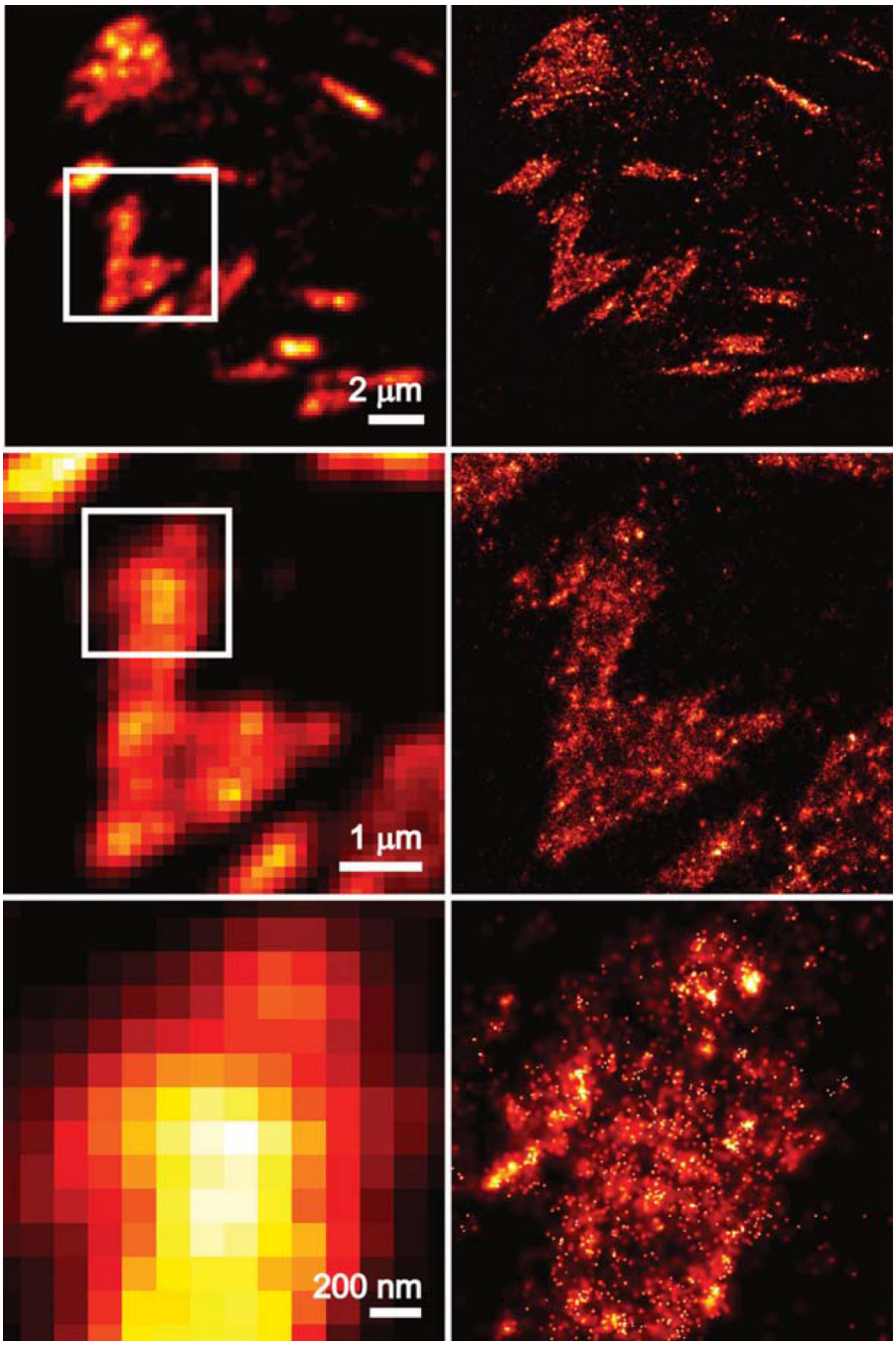

Figure 4.21.1.
Comparison between diffraction-limited, summed TIRF (left) and PALM (right) images of tdEos/vinculin distributions in adhesion complexes present at the surface of a fixed HFF-1 fibroblast. Middle/bottom panels show higher magnification views of the boxed regions in top/middle panels. Note the greatly increased resolution and dynamic range evident with PALM. Displayed images were rendered from 40,000 single-molecule images; > 100,000 molecules are plotted in each PALM image. For the color version of this figure, go to http://www.currentprotocols.com/protocol/cb0421.

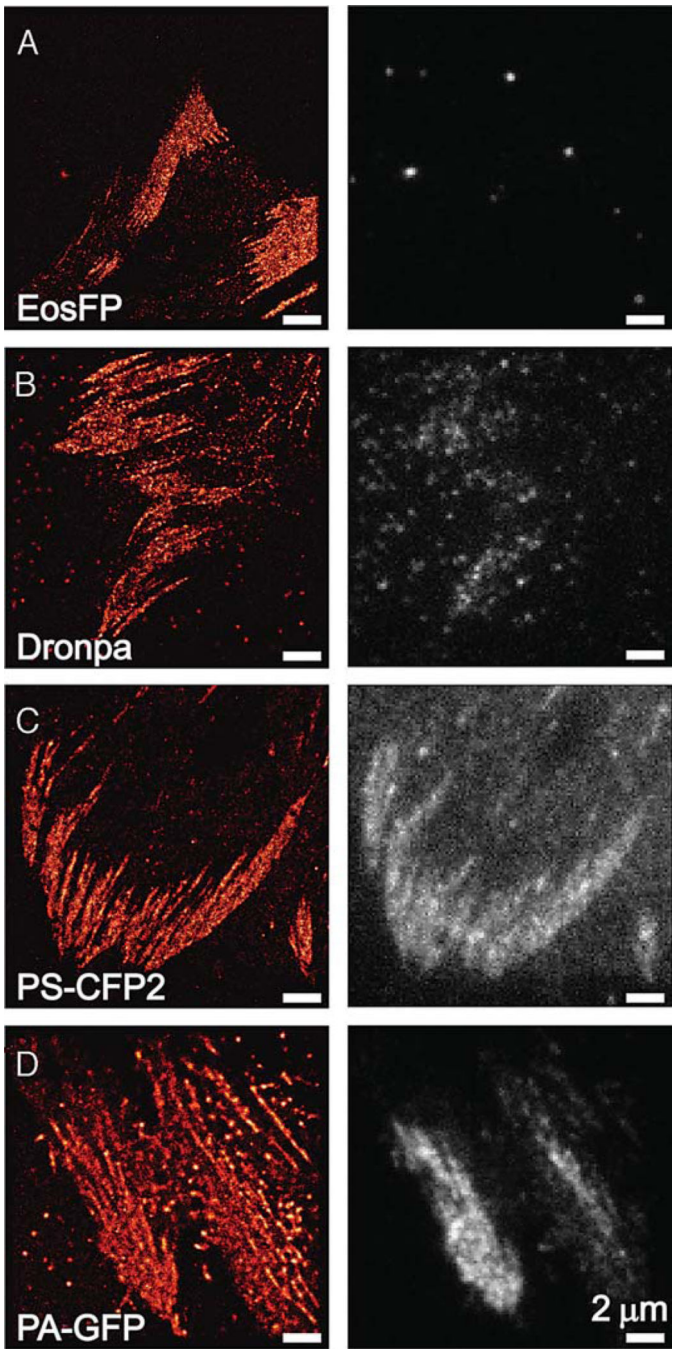

Figure 4.21.2.

Comparison of contrast ratios for four different PA-FPs, each fused to the adhesion protein paxillin. Left column tabulates PALM images obtained in each case: (**A**) mEosFP; (**B**) Dronpa; (**C**) PS-CFP2; (**D**) PA-GFP. Right column contains, for each PA-FP, frame 1000 of the stack of single-molecule images used to generate the corresponding PALM image on the left. Background largely reflects emission from the large pool of inactive PA-FPs. Note the correlation between low background (i.e., high contrast ratio between the active and inactive states) and crispness of the PALM image (i.e., localization precision). Reproduced from

Shroff et al., 2007. For the color version of this figure, go to http://www.currentprotocols.com/protocol/cb0421.

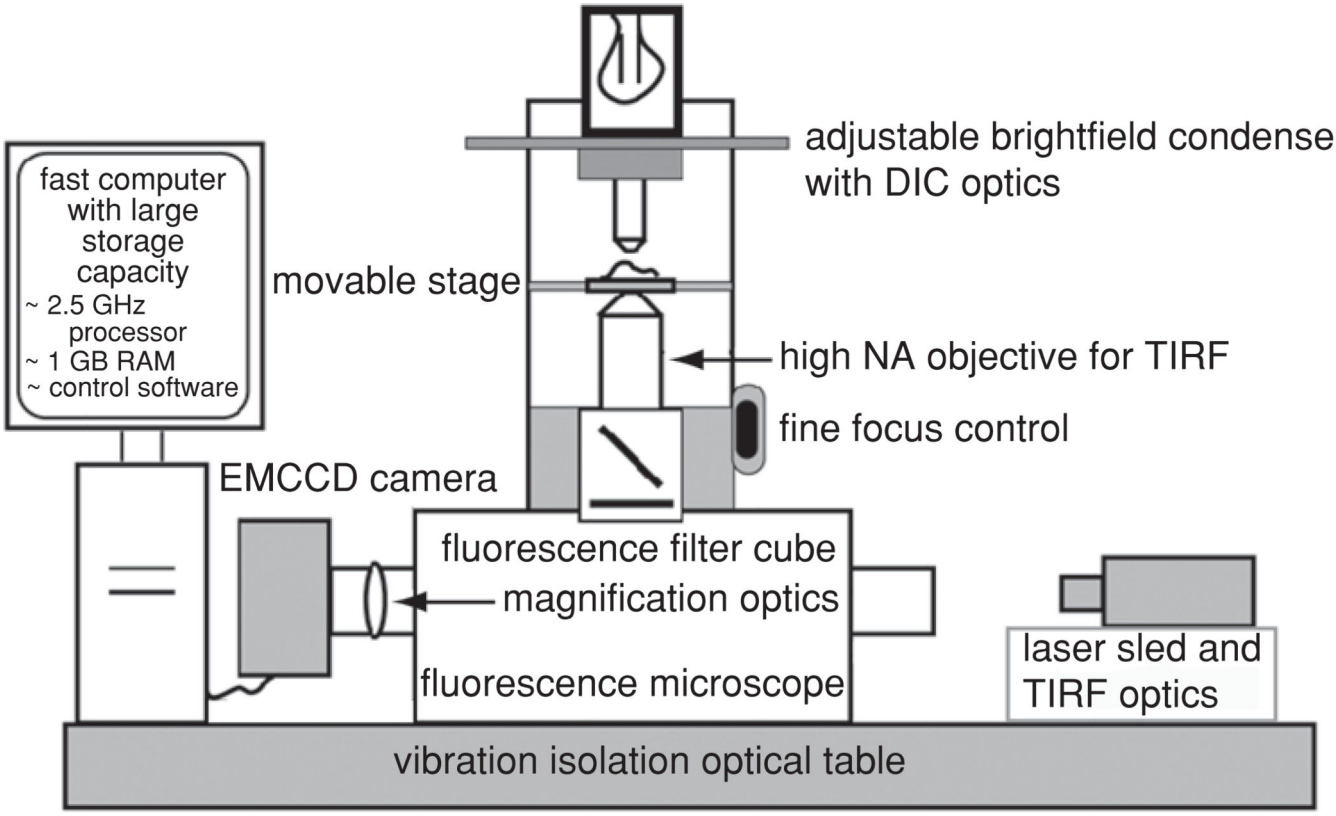

Figure 4.21.3.

Cartoon view of the main instrumentation components necessary for PALM. See the text for a detailed discussion of various components, and note that Figure 4.21.6 and Figure 4.21.7 show a detailed view of the sled and TIRF optics for coupling the excitation and activation lasers into the microscope body, while Figure 4.21.4 and Figure 4.21.5 show the sample holder and sample chamber (not shown in cartoon) in detail. The figure is not drawn to scale.

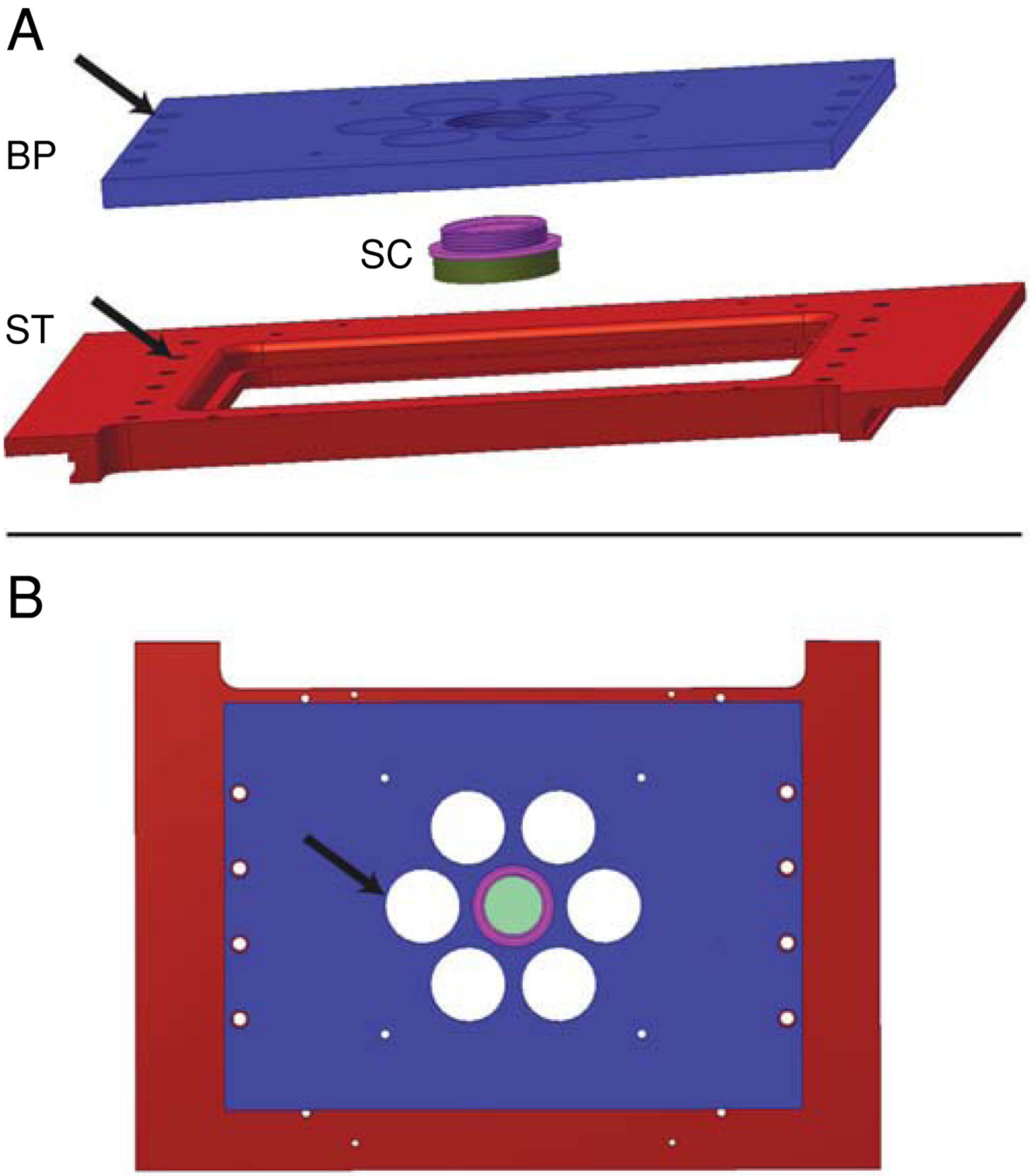

Figure 4.21.4.

Sample holder assembly. (**A**) The sample holder in PALM consists of a sample chamber assembly (SC, shown in more detail in Figure 4.21.5), that is threaded and fits into a top, steel baseplate (BP). The BP contains holes that are sized appropriately so that it can be bolted into the threaded holes of the ASI stage (ST) with appropriately threaded screws. Holes for bolting BP to ST are shown with arrows. (**B**) Bird's eye view of the sample holder. Additional access holes in BP (arrows) are useful for cleaning out old immersion oil from

the bottom surface of SC (as might accumulate with the high-index oil used with the 1.65 NA objective), while keeping the BP bolted to ST.

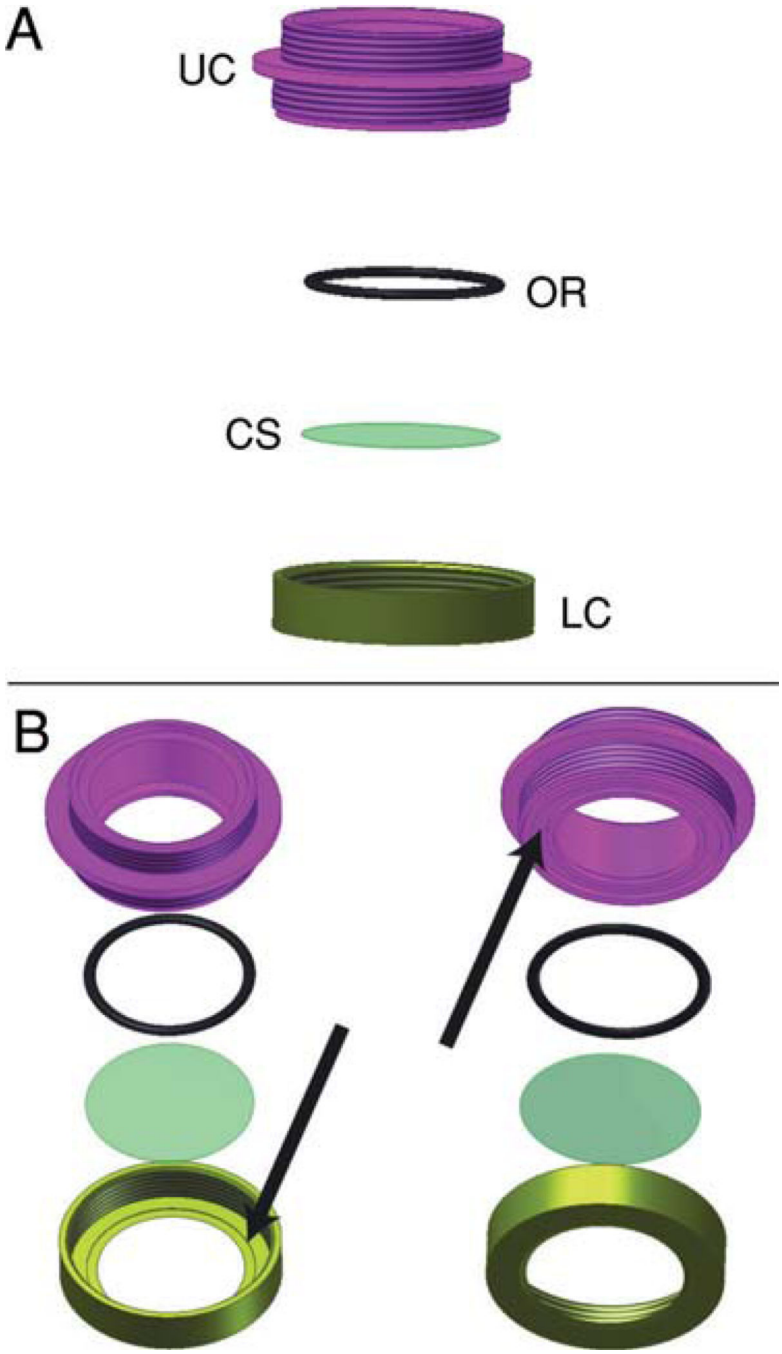

Figure 4.21.5.
Sample chamber assembly. (**A**) The sample chamber used in PALM consists of upper (UC) and lower (LC) steel assemblies that thread together. Between these two components are sandwiched the coverslip (CS) containing the sample, and an O-Ring (OR). OR prevents leaks when CS is immersed in buffer. (**B**) Different perspective view of the sample chamber assembly, with grooves in UC and LC for OR and CS indicated with arrows.

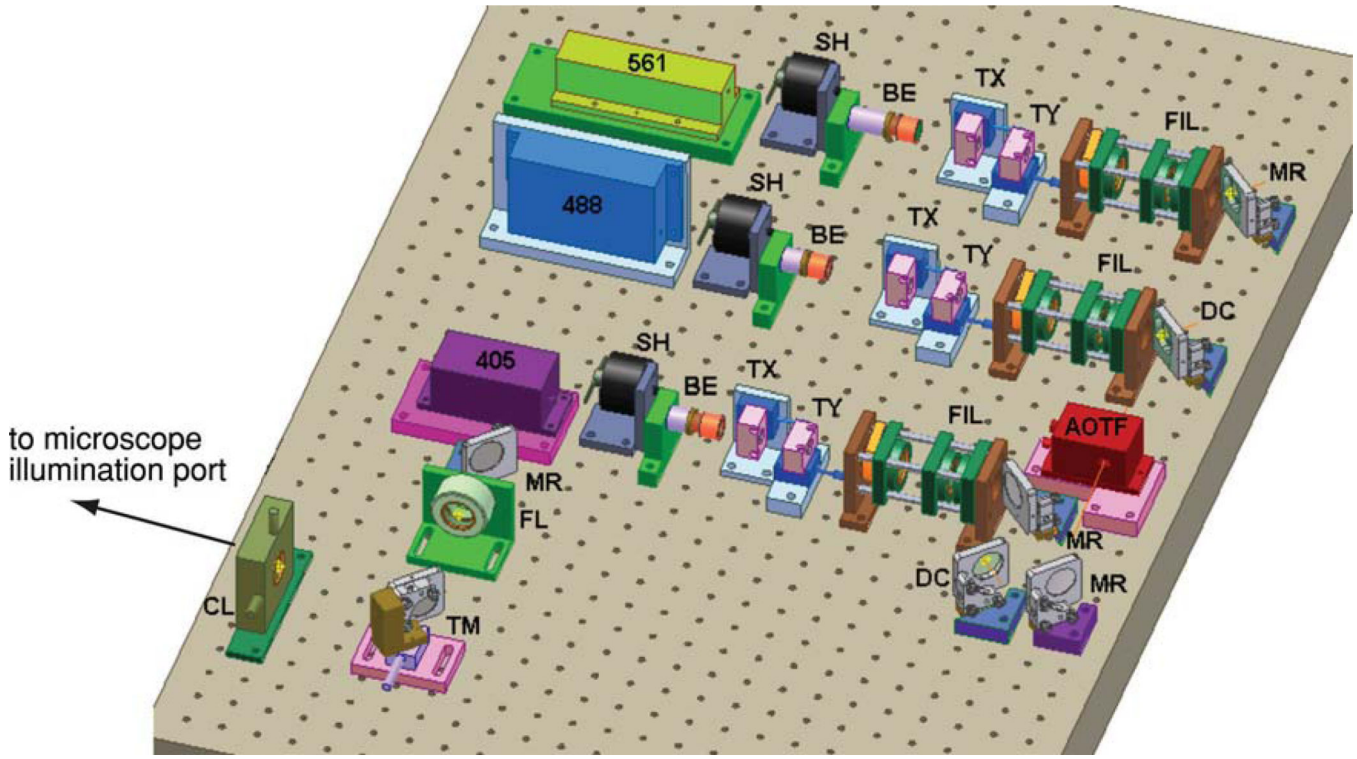

Figure 4.21.6.

Scheme for coupling excitation and activation light into the microscope for PALM. Lasers 488 and 561 excite the active forms of Dronpa and EosFP, respectively, and laser 405 converts each of these PA-FPs to the active form. The remaining elements are used to overlap the three lasers beams, adjust their diameters, and ensure their mutual propagation in a common direction (see text for a more detailed discussion). Symbol key: SH = shutter; BE = beam expander; TX =x direction beam translator; TY = y direction beam translator; FIL = filter group (wavelength, intensity, and polarization); MR = mirror; DC = dichroic beamsplitter; AOTF = acousto-optic tunable filter; FL = focusing lens; TM = translating mirror; CL = collimating lens. See the text in Basic Protocol 1 for discussion. Reproduced from Shroff et al., 2007.

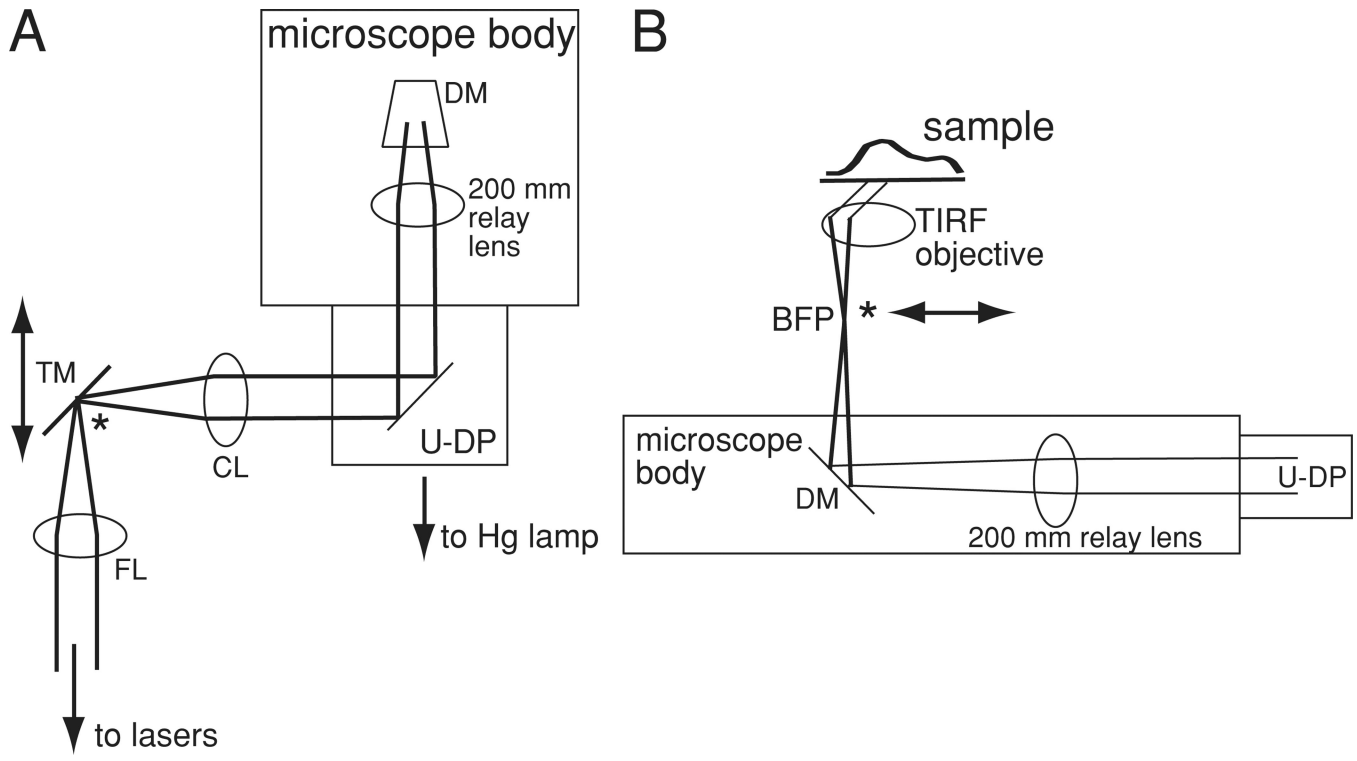

Figure 4.21.7.

Cartoon view of the optical path used for TIRF illumination. (**A**) Bird's eye view. Laser light is focused by lens FL, reflected from mirror TM, and recollimated by lens CL (note that these 3 optical elements are shown also in Figure 4.21.6). It enters the microscope back port via the Olympus U-DP attachment (used for switching between TIRF and mercury or xenon lamp illumination), whereby a single 200-mm relay lens (internal to the microscope body) focuses the light onto the back focal plane (BFP) of the objective, via the dichroic mirror (DM) in the filter cube assembly (not shown for clarity). (**B**) Side view of the light path after the U-DP. Light focused at the objective BFP emerges from the objective (shown as a single lens for clarity) as parallel rays, illuminating the sample at a critical angle in TIRF. Note that the focus at the BFP of the objective and the focus created between CL and FL are located in conjugate planes (indicated by the asterisks in the cartoon); translating TM thus serves to translate the focus at the BFP, allowing easy switching between epi- and TIRF configurations without changing the location of the illumination spot at the sample. See the text in Basic Protocol 1 for discussion.

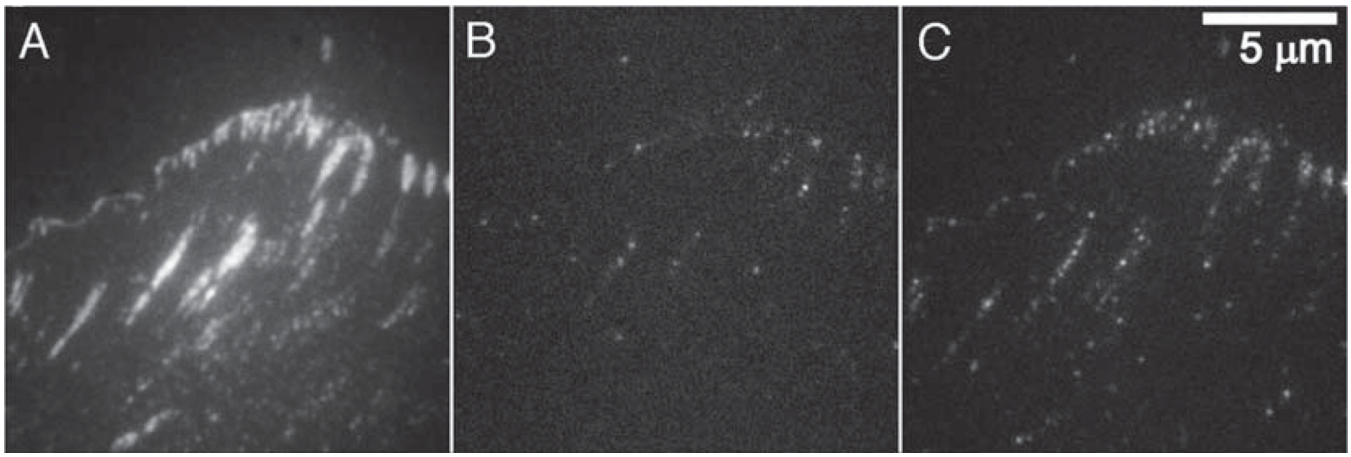

Figure 4.21.8.

The effect of different levels of activation power on single-molecule frames in a PALM acquisition. Images are of tdEos/paxillin molecules in adhesion complexes, and were taken with identical excitation power and exposure time, but differing levels of activation power. In (**A**), the activation power was too high: too many molecules were activated and thus it is difficult to discern individual molecules. The image appears diffraction limited, impeding the localization of single-molecules. In contrast, (**B**) displays a frame where the activation power was too low; consequently few molecules are excited and it will take longer than necessary to excite and bleach all tdEos molecules. The optimal activation power is illustrated in (**C**), where single-molecules are in close proximity but still resolvable. For the color version of this figure, go to http://www.currentprotocols.com/protocol/cb0421.

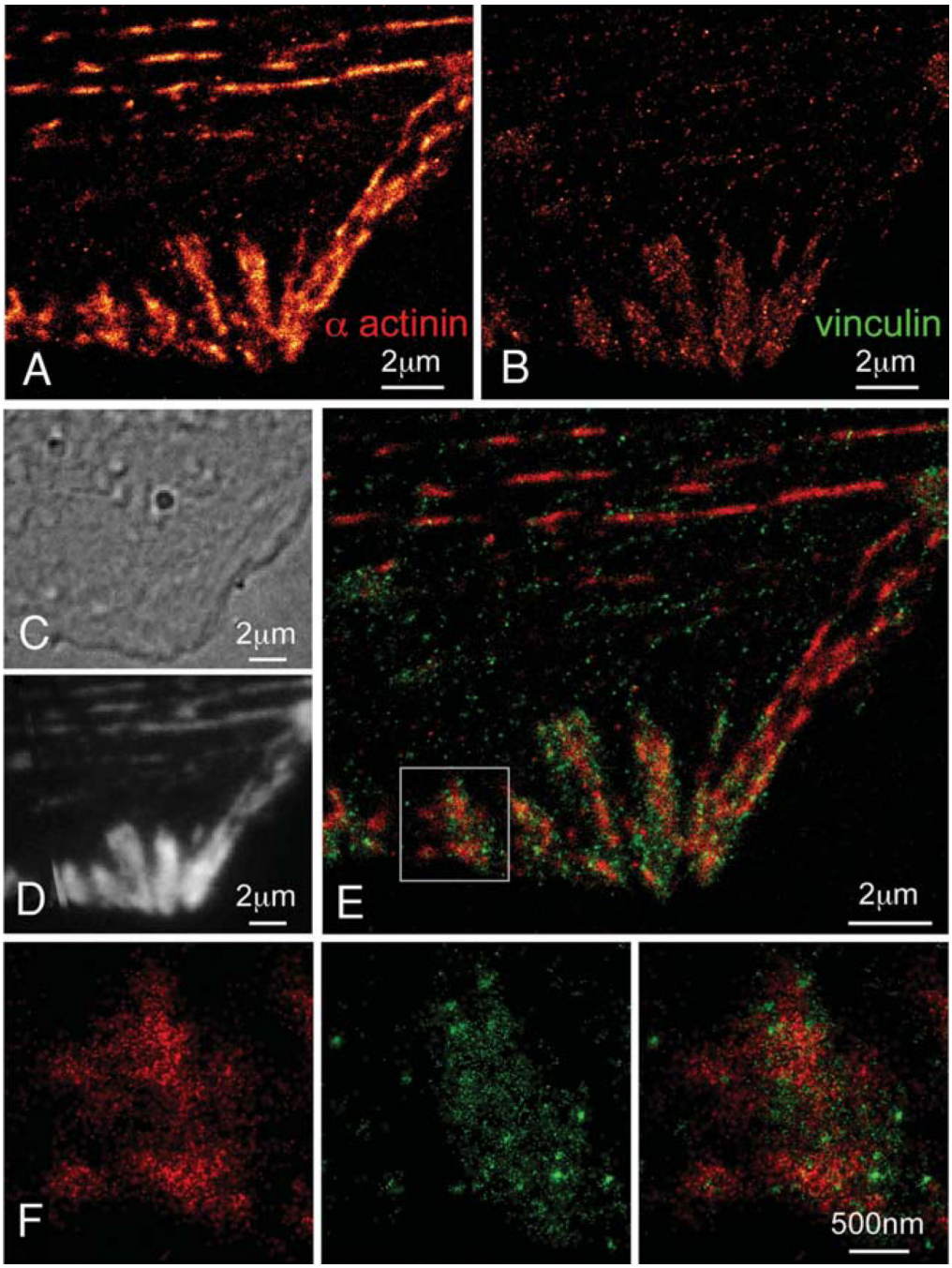

Figure 4.21.9.

Dual-color PALM image of tdEos/vinculin and Dronpa/α-actinin in a fixed HFF-1 cell: (**A**) PALM image of Dronpa-tagged α-actinin; (**B**) PALM image of tdEos-tagged vinculin; (**C**) DIC image revealing morphology; (**D**) TIRF image of combined tdEos and Dronpa emission (note the distinct morphologies of α-actinin and vinculin); (**E**) dual-color PALM overlay of α-actinin (red) and vinculin (green); (**F**) α-actinin, vinculin, and overlaid PALM images within the single adhesion shown in the box in (E). Panels (E) and (F) reveal that α-actinin and vinculin only partially co-localize within each adhesion complex, with α-actinin

existing in large patches emanating from stress fibers and vinculin coalescing in small, dense clusters scattered across each adhesion. Reproduced from Shroff et al., 2007. For the color version of this figure, go to http://www.currentprotocols.com/protocol/cb0421.

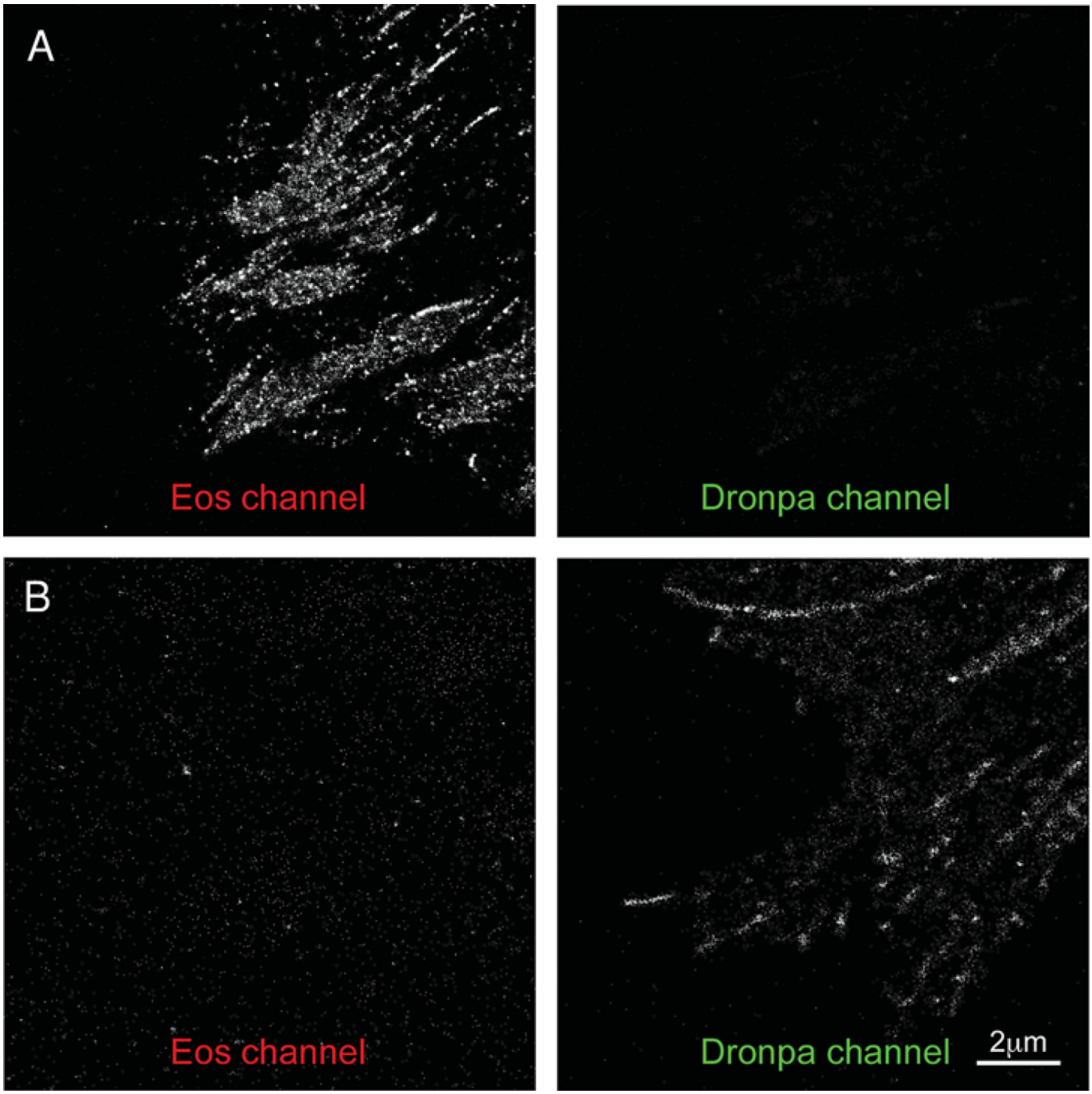

Figure 4.21.10.

Crosstalk control experiments. (**A**) Left: Eos channel PALM image of tdEos-tagged paxillin in an HFF-1 cell. Over 221,000 molecules were localized over 100,000 frames. Right: Dronpa channel PALM image of the same cell. 8900 molecules were localized over 50,000 frames. Note the negligible misidentification of Eos as Dronpa. (**B**) Left: Eos channel PALM image of Dronpa-tagged paxillin in an HFF-1 cell. 7800 molecules were localized over 50,000 frames. Right: Dronpa channel PALM image of the same cell. Over 22,000 molecules were localized over 8200 frames. The number of detected molecules in the Eos

channel in (B) is comparable to that found in untransfected control cells. In all cases, the Dronpa channel image was obtained after the EosFP channel image, and the images from both channels are plotted at identical brightness and contrast. Reproduced from Shroff et al., 2007.